

NONLINEAR MODEL REDUCTION VIA ADAPTIVE REDUCED BASES*

LIQIAN PENG[†] AND KAMRAN MOHSENI[‡]

Abstract. A new approach to model reduction of parameterized partial differential equations (PDEs) based on the concept of adaptive reduced bases is introduced. The presented approach is particularly suited for large-scale nonlinear systems characterized by parameter variations. Instead of approximating the solution of interest in a subspace spanned by global basis vectors, the proposed method approximates this solution in a lower-dimensional subspace generated by weighted snapshots, and each weighting coefficient is a function of the input parameter. Compared with global proper orthogonal decomposition, a more accurate approximating solution could be solved in a subspace with much fewer dimensions by the proposed method. Moreover, the corresponding reduced model can be formed by the discrete empirical interpolation method. Thus, the proposed method for nonlinear model order reduction is computationally efficient. The potential of the method for achieving large speedups while maintaining good accuracy is demonstrated for both elliptic and parabolic PDEs in two numerical examples.

1. Introduction. Due to computing speed barriers, in many engineering applications, direct numerical simulations are so computationally intensive that they either cannot be performed as often as needed or are more often performed in special circumstances than routinely. For this reason, during the past several decades, many efforts have been put forward to develop reduced models on time-critical operations such as electrical power grids [17], structural dynamics [1], chemical reaction systems [9], and CFD-based modelling and control [11, 19] to list a few. The core of model reduction is based on the fact that although the state of a complex system is in general represented by a large dimensional space, the linear subspace spanned by solution snapshots actually has a much lower dimension. To this effect, the proper orthogonal decomposition (POD) [11] or reduced basis methods [16] are developed to generate lower dimensional surrogates for the original large-scale complex problems. Although POD always looks for linear subspace instead of its curved submanifold, it is computationally tractable and able to capture the dominant patterns in a nonlinear system.

Compared with online dimensionality reduction methodology [17, 15], the offline-online splitting methodology is more often used in the real-time or many-query contexts to achieve minimal marginal cost per input-output evaluation. In the offline stage, the original problem corresponding to some sampled input parameters is solved to obtain some solution snapshots. For the online computation, a linear subspace for new input-output evaluation is constructed. To the best of our knowledge, there are at least three methods have been considered in the context of the reduced basis method: the global POD method, the local POD method and the adaptive POD method. The global POD method approximates the solution of interest in a subspace spanned by global basis vectors [21]. All the snapshots contribute equally to form the subspace. This method is straightforward for application, however, in order to obtain a high accuracy, a subspace with relatively high dimension should be used to construct the reduced model, especially when there exist many solution modes for

*This research was supported by the Office of Naval Research.

[†]Department of Mechanical and Aerospace Engineering, and Institute for Networked Autonomous Systems, University of Florida, Gainesville, FL, 32611-6250 (liqianpeng@ufl.edu).

[‡]Department of Mechanical and Aerospace Engineering, Department of Electrical and Computer Engineering, and Institute for Networked Autonomous Systems, University of Florida, Gainesville, FL, 32611-6250 (mohseni@ufl.edu).

the whole interested domain. Thus, global POD method inevitably keeps some redundant dimensions in the online computation and leads to long online simulation times. In order to form reduced model with significant lower dimension, local POD methods generate local reduced models by project the original equation onto a set of local reduced bases which corresponds to partial pre-computed snapshots. These snapshots are clustered through time domain partition [7], space domain partition [6] or parameter domain partition [8]. Local reduced models need less extra dimensions to present an approximating solution, but its solution cannot obtain a high order accuracy unless enough local data is given. The other method use global data, but form an adaptive reduced basis through an interpolation scheme. It could be directly computed by the subspace angle interpolation approach [14] or the interpolation in the tangent space of Grassmann manifold [2]. Although these adaptive POD interpolation methods could construct new a subspace for each new parameter, the dimension of all the pre-computed subspaces and the new subspace are fixed to a same value. Thus, there is no flexibility to change the new subspace dimension in order to balance the accuracy and the approximating error of reduced models. Moreover, the subspace interpolation process inevitably introduce some numerical error and the corresponding error bound is difficult to estimate.

Once a subspace is obtained, reduced models are typically constructed by Galerkin projection. However, the Galerkin approach is limited to the problems of linear equation or low-order polynomial nonlinearities. When a general nonlinearity is present, the cost to evaluate the projected nonlinear function still depends on the dimension of the original system, resulting in simulation times that hardly improve over the original system. To this effect, the empirical interpolation method [3, 10], and its variant, discrete empirical interpolation (DEIM) [5] were developed to approximate the original system by constructing surrogates for the nonlinear terms of the original equation using a data fitting approach that employs their values at a few indices and a set of pre-determined shape functions.

In this paper, we provide a new method to form an adaptive reduced model for the parameter variation. The dimension of the reduced model could be adaptively chosen to obtain a certain level of accuracy. The basis vectors are directly computed by singular value decomposition (SVD) of a weighted snapshot matrix, whose columns are defined as the pre-computed snapshots multiplies weighting coefficients, which are similar to the coefficients for direction interpolation of the solution snapshots in the parameter space. When a compact interpolation scheme is used, the subspace it generates is similar to the one from a local POD method. When all the coefficients in the information matrix are set equally, this method degenerates to a global POD method. When a noncompact scheme is used, such as radial basis function or inverse distance weighting, the subspace behaves similar to local POD when the dimension is low and similar to global POD when the dimension is high. We demonstrate that reduced equation corresponding to this subspace gives much higher accuracy than the global reduced model with the same subspace dimension. Furthermore, the adaptive reduced model could be formed by the POD-DEIM approach, and therefore it is very efficient.

The remainder of this article is organized as follows. In section 2 and 3, an overview of model reduction for parameterized PDEs and a general error analysis are presented. Section 4 briefly reviews the classical POD-Galerkin method and its variant POD-DEIM method. Then a general method for elliptic PDEs is discussed in section 5. After introduce the chord method, we apply the classical POD method

for model reduction. Then adaptive reduced bases is proposed in order to use fewer modes to approximate the original system. Section 6 extends the adaptive reduced model to parabolic PDEs. Finally, conclusions are offered in section 7.

2. Formulation of Parameterized PDEs. We consider both parabolic PDEs and elliptic PDEs in this section. By discretization (for example, using finite difference or finite element methods), an elliptic parameterized PDE for variable $u \in \mathbb{R}^n$ with input parameter $\mu \in \mathbb{R}^m$ can be expressed as an algebraic equation

$$(2.1) \quad f(\mu, u) = 0,$$

where $f : \mathcal{D} \times \mathcal{R} \rightarrow \mathbb{R}^n$ is a smooth function for $\mathcal{D} \subset \mathbb{R}^m$ and $\mathcal{R} \subset \mathbb{R}^n$. For any fixed input parameter $\mu \in \mathcal{D}$, we seek a solution $u = u(\mu) \in \mathcal{R}$, such that $f(\mu, u) = 0$ could be satisfied.

Parabolic PDEs are often used to describe dynamical systems with time dependent solutions. Let $\mathcal{I} = [0, T]$ denote the time domain and \mathcal{D} denote the parameter domain. By spatial discretization, the original parabolic PDE becomes an ordinary differential equation (ODE)

$$(2.2) \quad \dot{u} = f(t, \mu, u),$$

with an initial condition $u(0, \mu) = u_0$, where $f : \mathcal{I} \times \mathcal{D} \times \mathcal{R} \rightarrow \mathbb{R}^n$ denotes the discretized vector field. For any fixed $t \in \mathcal{I}$ and $\mu \in \mathcal{D}$, the state variable $u = u(t, \mu) \in \mathcal{R} \subset \mathbb{R}^n$ satisfies (2.2). By definition, $u(t, \mu)$ is a flow which gives an orbit in \mathbb{R}^n as t varies over \mathcal{I} for a fixed initial condition u_0 and a fixed input parameter $\mu \in \mathcal{D}$. The orbit contains a sequence of states (or state vectors) that follow from u_0 .

In this article we shall respectively refer (2.1) and (2.2) as discretized elliptic and parabolic PDEs, although they can represent more general parameterized PDEs. In order to use the same framework to study (2.1) and (2.2), we use τ to represent μ in (2.1) and to represent (t, μ) in (2.2). Let \mathcal{T} denote the input space, and $\mathcal{T} = \mathcal{D}$ or $\mathcal{T} = \mathcal{I} \times \mathcal{D}$. Then for both scenarios, $u(\tau)$ and $f(\tau, u)$ could be used to represent the solution snapshot and the vector field corresponding to $\tau \in \mathcal{T}$. It follows that (2.1) and (2.2) become $f(\tau, u) = 0$ and $\dot{u} = f(\tau, u)$ respectively.

An offline-online splitting scheme is used for the model reduction in this article. Let p denote the ensemble size. In the offline stage, $\{\tau_i\}_{i=1}^p$ are sampled in the parameter space, and the corresponding solutions with their derivatives could induce a subspace, where the real solution approximately resides. Induced subspaces in the context of model reduction include the Lagrange, Taylor and Hermite subspaces [16]. In this article, we are focusing on constructing a reduced model in the Lagrange subspace $\mathcal{S}_r = \text{span } \{u_i\}_{i=1}^p \subset \mathbb{R}^n$. The subspace \mathcal{S}_r belongs to the Grassmann manifold $\mathcal{G}_{n,r}$ which is defined as the set of all r -dimensional subspaces of \mathbb{R}^n . The dimension r satisfies $r \leq \min\{n, p\}$. Let $\Phi_r := [\varphi_1, \dots, \varphi_r]$ contains an orthonormal basis $\{\varphi_i\}_{i=1}^r$ of \mathcal{S}_r . Let superscript T denotes matrix transpose, and I_r is the $r \times r$ identity matrix. Then $\Phi_r \in \mathcal{V}_{n,r}$, where $\mathcal{V}_{n,r} = \{A \in \mathbb{R}^{n \times r} | A^T A = I_r\}$ is denoted as the Stiefel manifold of orthonormal r -frames in \mathbb{R}^n . When $r \approx n$, a reduced equation constructed in \mathcal{S}_r could not obtain significant speedups. One often seeks a $k (\ll r)$ -dimensional linear subspace $\mathcal{S}_k \subset \mathcal{S}_r$ where most solution vectors approximately reside. Moreover, there exists an $n \times k$ matrix $\Phi_k = [\phi_1, \dots, \phi_k] \in \mathcal{V}_{n,k}$ whose column space is \mathcal{S}_k . Once the subspace is specified, a reduced model can be constructed by several approaches, such as Galerkin projection [13], Petrov-Galerkin projection [4], and empirical interpolation [3, 10].

3. A General Error Analysis of Reduced Equations. Regardless of the techniques applied for model reduction, a key consideration is how to approximate the original system with high accuracy. In this section, we shall give a general error analysis for the projection-based reduced models.

Using the notations from the previous section, the projection of a state variable $u \in \mathbb{R}^n$ onto \mathcal{S}_r and \mathcal{S}_k can be respectively presented by $\tilde{u}_r := \Phi_r \Phi_r^T u$, and $\tilde{u}_k := \Phi_r \Phi_k^T u$. Let $e_r := u - \tilde{u}_r$ denote the difference between a solution vector u and its projection on \mathcal{S}_r , and $e_k := u - \tilde{u}_k$ denote the difference between u and its projection on \mathcal{S}_k . In addition, we define $e_o := \tilde{u}_r - \tilde{u}_k$ as the difference between these two projections of u .

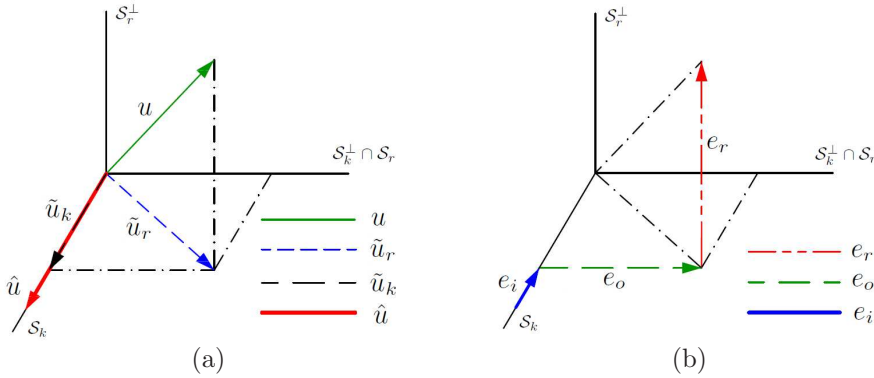


FIGURE 3.1. (Color online.) (a) Illustration of the actual solution u for the original system, the projection \tilde{u}_r of u on \mathcal{S}_r , the projection \tilde{u}_k of u on \mathcal{S}_k and the approximating solution \hat{u} computed by a reduced model. (b) The component of error orthogonal to \mathcal{S}_r is given by $e_r = u - \tilde{u}_r$, the difference of two projections of u is given by $e_o = \tilde{u}_r - \tilde{u}_k$, and the component of error parallel to \mathcal{S}_k is given by $e_i = \tilde{u}_k - \hat{u}$.

Suppose the reduced model has a unique solution, \hat{u} , and $\hat{u} = \hat{u}(\tau) \in \mathcal{S}_k$. Usually, $\tilde{u}_k \neq \hat{u}$, and we use $e_i := \tilde{u}_k - \hat{u}$ to represent their difference. Moreover, numerical simulation inevitably introduces further the numerical error e_t , such as discretization of time integration and the round-off error. This kind of error exists for both high dimensional and low dimensional simulations. However, for simplicity we assume the solution to the reduced model \hat{u} is obtainable by an accurate numerical scheme, and neglect e_t . Using \mathcal{S}_r^\perp and \mathcal{S}_k^\perp to represent the orthogonal complement of subspaces \mathcal{S}_r and \mathcal{S}_k of \mathbb{R}^n , figure 3.1(a) shows u , its projections \tilde{u}_r , \tilde{u}_k , and its approximation from a reduced model \hat{u} . Figure 3.1(b) shows the different components, e_r , e_o , e_i , of error from a reduced model, defined by $e := u - \hat{u}$.

LEMMA 3.1. *The total error e of the approximating solution \hat{u} from a reduced equation, can be decomposed into three components: $e = e_r + e_o + e_i$, and these components are orthogonal to each other.*

Proof. By the definitions of e , e_r , e_o , and e_i , we immediately obtain

$$(3.1) \quad e = u - \hat{u} = (u - \tilde{u}_r) + (\tilde{u}_r - \tilde{u}_k) + (\tilde{u}_k - \hat{u}) = e_r + e_o + e_i.$$

Since $\tilde{u}_r \in \mathcal{S}_r$, $\tilde{u}_k \in \mathcal{S}_k \subset \mathcal{S}_r$, we have $e_o = \tilde{u}_r - \tilde{u}_k \in \mathcal{S}_r$. It follows that there exists a vector $a \in \mathbb{R}^r$ such that $e_o = \Phi_r a$. On the other hand,

$$e_r = u - \tilde{u}_r = (I_r - \Phi_r \Phi_r^T) u.$$

Then the inner product gives

$$(3.2) \quad (e_o, e_r) = a^T \Phi_r^T (I_r - \Phi_r \Phi_r^T) u = a^T (\Phi_r^T - I_r \Phi_r^T) u = 0.$$

Since $\tilde{u}_k, \hat{u} \in \mathcal{S}_k$, one could write $e_i = \tilde{u}_k - \hat{u} = \Phi_k b$ for a vector $b \in \mathbb{R}^k$. Since $\mathcal{S}_k \subset \mathcal{S}_r$, it follows that $(\Phi_r \Phi_r^T) \Phi_k = \Phi_k$. Then the inner product gives

$$(3.3) \quad (e_i, e_r) = b^T \Phi_r^T (I_r - \Phi_r \Phi_r^T) u = b^T (\Phi_r^T - (\Phi_r \Phi_r^T \Phi_k)^T) u = 0.$$

Similarly, by the definition of \tilde{u}_k , we have

$$e_k = u - \tilde{u}_k = (I_k - \Phi_k \Phi_k^T) u.$$

Then the inner product gives

$$(3.4) \quad (e_i, e_k) = a^T \Phi_r^T (I_k - \Phi_k \Phi_k^T) u = a^T (\Phi_k^T - I_k \Phi_k^T) u = 0.$$

On the other hand,

$$(3.5) \quad e_k = u - \tilde{u}_k = u - \tilde{u}_r + \tilde{u}_r - \tilde{u}_k = e_r + e_o.$$

e_o could be considered as the projection of e_k onto the orthogonal complement of \mathcal{S}_k as a subspace of \mathcal{S}_r . Using (3.3), (3.4) and rewriting (3.5) as $e_o = e_k - e_r$, one obtains

$$(3.6) \quad (e_i, e_o) = (e_i, e_k - e_r) = (e_i, e_k) - (e_i, e_r) = 0.$$

A combination of (3.2), (3.3) and (3.6) concludes e_r, e_o, e_i are orthogonal to each other. Moreover, e_k and e_i are orthogonal to each other. \square

Decreasing the magnitude of the projection error $e_k (= e_r + e_o)$ is the key to decrease the total error $e (= e_k + e_i)$. On one hand, e_k provides a lower bound for the reduced model, as $\|e_k\| \leq \|e\|$ is always satisfied. On the other hand, for both elliptic [16] and parabolic PDEs [18], if the Galerkin method is used to produce the reduced equation, there respectively exist a constant C such that $\|e\| \leq C \|e_k\|$. Therefore, a upper error bound of e is also related to e_k . The first component e_r of e_k is directly related to sampling input parameters during the offline stage. One could use uniform sampling process in the parameter space, or use nonuniform sampling process through a greedy algorithm [3, 10]. The second component e_o of e_k comes from the error of dimensionality reduction. If the global POD method is used, then e_o is related to the truncation of SVD. In this article we are about to discuss an adaptive method to form a reduced subspace \mathcal{S}_k such that $\|e_o\|$ could reach a lower value with fixed k . We will begin with a brief review of POD, which pave a way to introduce the adaptive reduced model.

4. Proper Orthogonal Decomposition (POD). In this section, we give a brief overview of the procedure and properties of POD. In a finite dimensional space, it is essentially the same as the singular value decomposition (SVD). Let $X = [u_1, \dots, u_p]$ be a $n \times p$ snapshot matrix, where each column $u_i = u(\tau_i)$ represents a solution snapshot corresponding to input parameters τ_i . The POD method constructs a basis matrix $\Phi_k \in \mathcal{V}_{n,k}$ that solves the following minimization problem

$$(4.1) \quad \min_{\Phi_k \in \mathcal{V}_{n,k}} \|(I - \Phi_k \Phi_k^T) X\|_F.$$

Thus, the basis matrix Φ_k minimizes the Frobenius norm of the difference between X with its projection $\tilde{X} := \Phi_k \Phi_k^T X$ onto \mathcal{S}_k . Since the dimension of the Lagrange subspace \mathcal{S} is r , it follows that $\text{rank}(X) = r$. Thus, the SVD of X gives

$$(4.2) \quad X = V \Lambda W^T,$$

where $V \in \mathcal{V}_{n,r}$, $W \in \mathcal{V}_{p,r}$, and $\Lambda = \text{diag}(\lambda_1, \dots, \lambda_r) \in \mathbb{R}^{r \times r}$ with $\lambda_1 \geq \lambda_2 \geq \dots \geq \lambda_r > 0$. The λ s are called the singular values of X . In many applications, the truncated SVD is more economical, where only the first k columns V' of V and the first k columns W' of W corresponding to the diagonal matrix Λ' corresponding to the k largest singular values are calculated, and the rest of the matrix is not computed. Then the projection of X is given by

$$(4.3) \quad \tilde{X} = V' \Lambda' W'^T,$$

and the solution of Φ_k in (4.1) is given by $\Phi_k = V'$. Moreover, the projection error of (4.1) in Frobenius norm by the POD method is given by

$$(4.4) \quad E_k = \|(I - \Phi_k \Phi_k^T) X\|_F = \sqrt{\sum_{i=k+1}^r \lambda_i^2}.$$

The key of POD and other projection based reduced models is to find a k -dimensional subspace \mathcal{S}_k on which all the state vectors live. Although the truncated SVD is no longer an exact decomposition of the original matrix X , but it provides the best approximation \tilde{X} to the original data X with least Frobenius norm under the constraint that $\dim(\tilde{X}) = k$. In the rest of this paper, SVD refers to truncated SVD unless specified otherwise.

4.1. Galerkin Projection. Let $v_k \in \mathbb{R}^k$ denote the state variable in the subspace coordinate system, and $\hat{u}_k = \Phi_k v_k$ denote the same state in the original coordinate system. Projecting the system (2.1) onto \mathcal{S}_k , one obtains the reduced model of an elliptic PDE,

$$(4.5) \quad \Phi_k^T f(\tau, \Phi_k v_k) = 0,$$

where $\tau = \mu \in \mathcal{D}$ denotes the input parameter. Analogously, a reduced model of a parabolic PDE can be obtained by projecting the system (2.2) on to \mathcal{S}_k ,

$$(4.6) \quad \dot{v}_k = \Phi_k^T f(\tau, \Phi_k v_k),$$

and $\tau = (t, \mu) \in \mathcal{I} \times \mathcal{D}$ is used to identify the solution trajectory corresponding to μ at time t .

Equations (4.5) and (4.6) are reduced equations formed by Galerkin projection. In fact, they can achieve fast computation only when the analytical formula of the reduced vector field $\Phi_k^T f(\tau, \Phi_k v_k)$ can be significantly simplified, especially when it is a linear (or a polynomial) function of v . Otherwise, one need to compute the state variable in the original system $\Phi_k v$, evaluate the nonlinear vector field f at each element, and then, project f onto \mathcal{S}_k . In this case, the reduced models (4.5) and (4.6) are more expensive than the correspondingly full models. To this effect, the discrete empirical interpolation method (DEIM) [5] is proposed to decrease the complexity of computing the nonlinear vector field.

4.2. Discrete Empirical Interpolation Method (DEIM). The original vector field, $f(\tau, u)$ can be split into a linear part and a nonlinear part, i.e.,

$$(4.7) \quad f(\tau, u) = L(\tau)u + N(\tau, u).$$

Using the Galerkin projection, the reduced vector field can be written as

$$(4.8) \quad \Phi_k^T f(\tau, \Phi_k v_k) = \hat{L}v_k + \Phi_k^T N(\tau, \Phi_k v_k),$$

where $\hat{L}(\tau) = \Phi_k^T L \Phi_k$ is a linear operator and $\Phi_k^T N(\tau, \Phi_k v_k)$ denotes the nonlinear term of the vector field. Unless the nonlinear term can be analytically simplified, its computational complexity still depends on n . An effective way to overcome this difficulty is to approximate the nonlinear term by projecting it onto a subspace with much lower dimension. Considering u is a smooth function of τ , we can define a *nonlinear snapshot* $g(\tau) =: N(\tau, u(\tau))$ for $\tau \in \mathcal{T}$. Then the reduced vector field from (4.7) restricted on $\tau \in \mathcal{T}$ and $u = u(\tau)$ can be approximated as

$$(4.9) \quad \Phi_k^T f(\tau, u(\tau)) = \hat{L}v_k + [\Phi_k^T \Psi(P^T \Psi)^{-1}][P^T g(\tau)],$$

where Ψ denotes the collateral POD basis based on a pre-computed nonlinear snapshot ensemble, and P^T is the index matrix to project a vector of dimension n onto its l elements. For example, if $a = [a_1, \dots, a_4]^T$, and $P^T = [1 \ 0 \ 0 \ 0; 0 \ 0 \ 1 \ 0]$, then $P^T a = [a_1, a_3]$. P can be computed by an offline greedy algorithm. We recommend readers to refer [5] for more details. Notice that $\Phi_k^T \Psi(P^T \Psi)^{-1}$ is calculated only once at the beginning and $P^T g(\tau)$ is only evaluated on l elements of $g(\tau)$, therefore it is very efficient when $l \ll n$. Using the POD-DEIM approach, we will respectively study nonlinear elliptic and parabolic PDEs in the next two sections.

5. Nonlinear Elliptic PDEs. We are focusing on model reduction for elliptic nonlinear PDEs in this section. The algorithms in this section could be considered as an order-reduced extension for the chord method. We follow the offline-online splitting computational strategy, and use the discrete empirical interpolation method (DEIM) to treat nonlinear terms in the original system.

The general form of parabolic PDEs, after discretization, is given by a nonlinear algebraic equations (2.1). Let p denote the ensemble size. In the offline stage, $\{\mu_i\}_{i=1}^p$ are sampled in the parameter space, and we solve the corresponding solutions $\{u_i\}_{i=1}^p$. If $u_i = u(\mu_i)$ satisfies (2.1), and the Jacobian matrix $J_i := D_u f(\mu_i, u_i)$ is nonsingular, then by the implicit function theorem, there exists neighborhoods $V_i \subset \mathbb{R}^m$ of μ_i , and $U_i \subset \mathbb{R}^n$ of u_i and a smooth map $u : V_i \rightarrow U_i$ such that locally, (2.1) has a unique solution. For a new fixed parameter $\mu_* \in \cap_i V_i$, the following equation has a unique solution,

$$(5.1) \quad F(u) = 0,$$

where $F(u) := f(\mu_*, u)$. Newton iteration and its variations are the most efficient methods known for solving systems of non-linear equations. The most expensive procedures of the standard Newton iteration are to compute the $n \times n$ Jacobian matrix F' for each iteration. Unless an analytical form of F' could be obtained explicitly, evaluation of F' by finite difference method costs n times an evaluation of F because each column in F' requires an evaluation of F .

Motivated by this fact, chord iteration computes $J_0 = F'(u(0))$ at the outset, and use J_0 to approximate the Jacobian for each iteration. Specifically, for iteration j , we

first compute the vector $F(u(j))$. Then, solve

$$(5.2) \quad J_0 \xi(j) = -F(u(j))$$

for $\xi(j)$. After that, update the approximating solution,

$$(5.3) \quad u(j+1) = u(j) + \xi(j).$$

Under certain conditions, the chord iteration could obtain a convergent solution if the initial trial solution is close enough to the actual solution, as given by the following theorems.

THEOREM 5.1. *Suppose (5.1) has a solution u_* , F' is Lipschitz continuous with Lipschitz constant γ , and $F'(u_*)$ is nonsingular. Then there are $\bar{K} > 0$, $\delta > 0$, and δ_1 such that if $u(j) \in \mathcal{B}_{u_*}(\delta)$ and $\|\Delta(u(j))\| < \delta_1$ then*

$$(5.4) \quad u(j+1) = u(j) - (F'(u(j)) + \Delta(u(j)))^{-1}(F(u(j)) + \epsilon(u(j)))$$

is defined and satisfies

$$(5.5) \quad \|e(j+1)\| \leq \bar{K}(\|e(j)\|^2 + \|\Delta(u(j))\| \|e(j)\| + \|\epsilon(u(j))\|),$$

where $e(j) := u_* - u(j)$ denotes the error for iteration j .

For chord iteration, $\epsilon(u(j)) = 0$, $\Delta(u(j)) = F'(u_0) - F'(u(j))$. If $u_0, u(j) \in \mathcal{B}_{u_*}(\delta)$, $\|\Delta(u(j))\| \leq \gamma \|u_0 - u(j)\| \leq \gamma (\|e(0)\| + \|e(j)\|)$. Using theorem 5.1, the following theorem is obtained, where $K_C := \bar{K}(1 + 2\gamma)$.

THEOREM 5.2. *Let the assumptions of theorem 5.1 hold. Then there are $K_C > 0$ and $\delta > 0$ such that if $u_0 \in \mathcal{B}_{u_*}(\delta)$ the chord iteration converges linearly to u_* and*

$$(5.6) \quad \|e(j+1)\| \leq K_C \|e(0)\| \|e(j)\|.$$

We suggest readers to refer to [12] for proofs and more details. For chord method, the complexity of (5.2), (5.3), and direct evaluating $F(u)$ depends on n . If the dimension n in (5.1) is very large, chord iteration could be still prohibitively expensive for real time computation. For this reason, a model reduction approach is applied for decreasing the computational cost based on chord method. A manifold learning procedure is used to extract information from the original data. Usually, this procedure is very intensive in exchange for greatly decreased online cost for each new input-output evaluation. In the online stage, a reduced version of the chord method is used to solve for solution. Since the solution can be solved in a low dimensional subspace, the complexity of online computation can be very low.

5.1. Model Reduction for Chord Iteration. In the offline stage, for each input μ_i , the solution snapshot u_i , the nonlinear snapshot g_i , and the corresponding Jacobian matrix J_i are recorded to form an ensemble $\{\mu_i, u_i, g_i, J_i\}_{i=1}^p$. In the offline stage, we can use POD-Galerkin approach or POD-DEIM to accelerate the computation.

As described in section 4, using SVD, we can obtain the POD basis matrix Φ_k for the solution snapshots $X = [u_1, \dots, u_p]$ and collateral basis matrix Ψ for the nonlinear snapshots $X' = [g_1, \dots, g_p]$. Let $v(j) \in \mathbb{R}^k$ be the reduced state at iteration j , $J_0 = F'(u_0)$ be the of Jacobian at the trial solution, $\hat{J}_0 = \Phi_k^T J_0 \Phi_k \in \mathbb{R}^{k \times k}$ be

the projection of Jacobian J_0 onto \mathcal{S}_k . The Galerkin projection can be used to form reduced equations for (5.2) and (5.3) in chord method,

$$(5.7) \quad \hat{J}_0 \hat{\xi}(j) = -\Phi_k^T F(\Phi_k v(j)),$$

$$(5.8) \quad v(j+1) = v(j) + \hat{\xi}(j).$$

When J_0 is a symmetric positive definite (SPD) matrix, \hat{J}_0 is a nonsingular matrix and (5.7) is well-defined [20]. Moreover, it minimizes the mean square error in the search direction for each iteration. Unfortunately, the Jacobians of a nonlinear problem are not in general SPD matrices and \hat{J}_0 defined above could be singular. One efficient way is to partition the whole parameter domain into some subdomains. For one subdomain, one could pick one parameter, say μ_q , in $\{\mu_i\}_{i=1}^p$ and compute the Jacobian J_q as well as its projection \hat{J}_q onto J_k . If \hat{J}_q is (near) singular, one can choose another parameter in the same subdomain and the reduced Jacobian is nonsingular. Consequently, in the oneline stage, one can directly set \hat{J}_0 from the recorded $\{\hat{J}_q\}$ in the ensemble.

As mentioned in the previous section, POD-Galerkin approach cannot effectively reduce the complexity for high dimensional systems when a general nonlinearity is present, since the cost of computing $\Phi_k^T F(\Phi_k v)$ depends on the dimension of the original system. In order to obtain significant speedups for a general nonlinear system, the DEIM is used to form the reduced version of chord iteration, as shown in algorithm 1. An ensemble $\{\mu_i, u_i, g_i, J_i\}_{i=1}^p$ is pre-computed offline. The POD basis and the collateral POD basis are respectively computed in steps 1 and 2. Some matrices for DEIM is pre-computed in step 3. Step 4 involves parameter domain partition. We use uniform partition in the following simulations. But the algorithm here does not preclude nonuniform partitions. For each subdomain, we choose a reference parameter μ_q and compute and the reduced Jacobian \hat{J}_q and the reduced state v_q .

In the online stage, step 6 requires computing the distance from new input parameter μ_* to each reference parameters in the ensemble. Typically the dimension of parameter space is much lower than the dimension of state variable. In this case, this step is very cheap. Step 7 simply picks up the trial solution and the estimated Jacobian computed in step 5 during the offline stage. Step 6 and 7 are carried out only once. Steps 8-10 in the main loop are carried out in the subspace and their complexity is independent of n . Therefore, the online computation of algorithm 1 is very efficient.

Fixed τ in (4.5), the reduced algebraic equation formed by the Galerkin projection is given by

$$(5.9) \quad \Phi_k^T F(\Phi_k v) = 0.$$

Usually, the reduced chord iteration could not converges to the actual solution, v_* , of (5.9) since DEIM provides an extra error for the approximation for the vector field. However, suppose the DIEM approximation gives a uniform error bound, ϵ_F , for an interested domain of u , an error bound of algorithm 1 could be obtained in terms of ϵ_F . We slightly abuse the notation and use e to dentate the error between v_* and the approximating solution in reduced chord iteration.

THEOREM 5.3. *Suppose (5.9) has a solution v_* , F' is Lipschitz continuous with Lipschitz constant γ , and $F'(\Phi_k v_*)$ is nonsingular. The DIEM approximation gives*

Algorithm 1 Reduced Chord method

Require: Pre-computed ensemble $\{\mu_i, u_i, g_i, J_i\}_{i=1}^p$.

Ensure: Solution u_* that satisfies $F(u) = 0$.

Offline:

- 1: Use SVD to compute the global POD basis Φ_k for solution snapshots $\{u_i\}_{i=1}^p$.
- 2: Use the SVD to compute the globally collateral POD basis Ψ for nonlinear term $\{g_i\}_{i=1}^p$.
- 3: Use the DEIM to compute $\tilde{L} = \Phi_k^T L \Phi_k$ for linear operator and $\Phi_k^T \Psi (P^T \Psi)^{-1}$ for nonlinear term.
- 4: Partition the parameter space into p' subdomains.
- 5: For each subdomain, choose a reference parameter μ_q such that reduced Jacobian $\hat{J}_q = \Phi_k^T J_q \Phi_k$ is nonsingular. Compute solution snapshots in the reduced coordinate system $v_q = \Phi_k^T u_q$.

Online:

- 6: In the parameter space, compute the distance $d_q = \|\mu_* - \mu_q\|$ from the new parameter μ_* to each reference parameter μ_q .
- 7: Pick up μ_q with minimal distance, and set v_q as the initially trial solution $v(0)$ in the reduced coordinate system and set \hat{J}_q as the approximation of Jacobian \hat{J}_0 .
- for** $j = 0, \dots$, (until convergence) **do**

 - 8: Compute $\Phi_k^T \hat{F}(\Phi_k v(j))$, where \hat{F} is an approximation of F by DEIM.
 - 9: Solve $\hat{J}_0 \hat{\xi}(j) = -\Phi_k^T F(\Phi_k v(j))$, as (5.7).
 - 10: Update $v(j+1) = v(j) + \hat{\xi}(j)$, as (5.8).

- end for**
- 11: Set $\hat{u}_* = \Phi_k v(j+1)$.

a uniform error bound $\|F(u) - \hat{F}(u)\| < \epsilon_F$ for any $u \in \mathcal{B}_{\Phi_k v_*}$, then there are $\bar{K} > 0$, $K_C > 0$, $\delta > 0$ such that if $u_q \in \mathcal{B}_{\Phi_k v_*}(\delta)$ the reduced chord iteration approach to v_* with the error bound of $\|e(j)\|$ given by $\bar{K} \varepsilon_F / (1 - K_C \delta)$ as $j \rightarrow \infty$ where $e(j) := v_* - v(j)$ denotes the error for iteration j .

Proof. In algorithm 1, a sequence $\{v(j)\}$ is obtained by the following iteration rule,

$$(5.10) \quad v(j+1) = v(j) - \hat{J}_0^{-1}(\Phi_k^T \hat{F}(\Phi_k v(j))),$$

where $\hat{J}_0 = \Phi_k^T J_q \Phi_k$ for $J_q = F'(u_q)$. The above equation could be rewritten in the form similar to (5.4),

$$(5.11) \quad v(j+1) = v(j) - (\Phi_k^T F'(\Phi_k^T v(j)) + \Delta(v(j)))^{-1}(\Phi_k^T F(\Phi_k v(j)) + \epsilon(v(j))),$$

where $\epsilon(v(j)) = \Phi_k^T \hat{F}(\Phi_k v(j)) - \Phi_k^T F(\Phi_k v(j))$, and $\Delta(v(j)) = \hat{J}_0 - \Phi_k^T F'(\Phi_k v(j)) \Phi_k$.

If $u_q, \Phi_k v(j) \in \mathcal{B}_{u_*}(\delta)$, one obtains $\|\epsilon(v(j))\| \leq \|\hat{F}(\Phi_k v(j)) - F(\Phi_k v(j))\| < \epsilon_F$, and $\|\Delta(v(j))\| \leq \|F'(u_q) - F'(\Phi_k v(j))\| \leq \gamma(\|e_q\| + \|e(j)\|)$. Using theorem 5.1, and define $K_C := \bar{K}(1 + 2\gamma)$, one obtains

$$(5.12) \quad \|e(j+1)\| < \bar{K} \|e(j)\| (\gamma \|e_q\| + (1 + \gamma) \|e(j)\|) + \bar{K} \varepsilon_F \leq K_C \delta \|e(j)\| + \bar{K} \varepsilon_F.$$

Let δ small enough such that $K_C \delta < 1$. It follows that $\|e(j)\|$ is bounded by $\bar{K} \varepsilon_F / (1 - K_C \delta)$ as $j \rightarrow \infty$. \square

The reduced chord iteration inherits one advantage of the standard chord iteration, i.e., it does not need compute the Jacobian at each iteration. Therefore, the

per-iteration cost of this method is lower than the cost from a reduced model formed by Newton iteration. On the other hand, an reduced Newton iteration cannot has quadratic convergence rate since the approximation error of the Jacobian matrix or the vector field is inevitable. Therefore, the reduced chord iteration is more efficient for solving the large-scale nonlinear algebraic equation in the context of on line computation.

Notice that if the error bound of DEIM approximation, ε_F in (5.12), approaches zero, the reduced chord iteration converges linearly to v_* . Moreover, ε_F is bounded by a constant times $\|(I - \Psi\Psi^T)F\|$ [5], which indicates an optimal collateral subspace is desired to decrease ε_F . For a fixed dimension k , the following section discuss how to generate optimal subspaces for the solution snapshots and the nonlinear snapshots.

5.2. Adaptive Reduced Model. We consider three SVD-based approaches to construct a subspace \mathcal{S}_k from \mathcal{S}_r . The first approach is the standard POD method, which constructs a *global reduced model* (GRM) from all the solution snapshots in the ensemble. Defining a matrix of p snapshots

$$(5.13) \quad X = [u_1, \dots, u_p],$$

then \mathcal{S}_k is spanned by the columns of the POD basis matrix Φ_k . The projection error of X in Frobenius norm is given by (4.4). This method is straightforward for application, however, if the problem depends on many parameters or if the solution shows a high variability with the parameters, a relatively high dimensional reduced space is needed in order to represent all possible solution variations well. This effect is even considerably increased when treating evolution problems with significant solution variations in time. Another aspect is the fact that projection based model reduction techniques, such as POD, usually generate small but full matrices while common discretization techniques (such as finite difference) could lead to large but sparse matrices. Unless the reduced model has significantly lower dimension, it is even possible that the reduced model is more time consuming than the original model.

The second approach is the *local reduced model* (LRM), which partitions the interested parameter domain into some disjoint regions and forms a local snapshot matrix for each region. Suppose μ_* resides on a region that contains l input parameters $\{\mu_i | i \in \mathcal{D}^L\}$ in the ensemble, where $\mathcal{D}^L = \{k_1, k_2, \dots, k_l\} \subset \{1, 2, \dots, p\}$, then the local snapshot matrix can be set as

$$(5.14) \quad X^L = [u_{k_1}, \dots, u_{k_l}].$$

The supper script L denotes the LRM. Since X^L contains less snapshots than X , it is expected that the LRM needs lower dimension to approximate the original system. Or equivalently, if the LRM has the same dimension as the GRM, it has less truncation error during the SVD process. On the other hand, since the LRM does not use solution snapshots in some other partitioned regions, it may not be able to obtain an approximating solution with high-order accuracy.

We extend the idea of the LRM and propose the third approach for model reduction, the *adaptive reduced model* (ARM), to compute the adaptive reduced bases for parameter variation. Similar to LRM, we first partition the interested parameter domain into some regions, and determine one region that μ_* resides. The reference solution snapshot u_q for this region could be approximated by a linear combination $u_q \approx \sum_{i=1}^p a_i(\mu_q)u_i$ of all the solution snapshots in the ensemble, where the interpolation coefficient $a_i(\mu_q)$ is a function on the parameter space, and satisfies $0 \leq a_i \leq 1$.

For example, it could be set as a Gaussian function $a_i(\mu_q) = C_0 \exp(-\|\mu_i - \mu_q\|^2/2\sigma^2)$, with the normalized coefficients C_0 and the kernel length σ . σ should be larger than the maximal radius of all the regions.

If μ_q is a close enough to μ_* , we can estimate an approximation of $u(\mu_*)$, or its projection \tilde{u}_r , through a variation of μ_q

$$(5.15) \quad \tilde{u}_r^A = \sum_{i=1}^p (1 + \eta_i) a_i u_i,$$

where $[\eta_1, \dots, \eta_p]^T \in \mathcal{B}_0(\epsilon_\eta)$, and $\eta_i = 0$ for all i if $a_i = 0$. We therefore can form a lower dimensional Lagrange subspace \mathcal{S}_r^A by $\{a_i u_i\}_{i=1}^p$ in \mathcal{S}_r . Using superscript A to denote the proposed ARM, a weighted snapshot matrix for the region that μ_* resides can be defined as

$$(5.16) \quad X^A = [a_1 u_1, a_2 u_2, \dots, a_p u_p].$$

Let $r^A = \det(X^A)$, obviously we have $r^A \leq r$. When $r^A > k$, the SVD can be used to extract the first k dominant modes from X^A , and obtain a subspace \mathcal{S}_k^A in \mathcal{S}_r^A . Let column vectors of $\Phi_k^A \in \mathcal{V}_{n \times k}$ span \mathcal{S}_k^A . As an analogy of E_k in (4.4), the projection error of X^A onto \mathcal{S}_k^A in Frobenius norm is given by

$$(5.17) \quad E_k^A = \left\| (I_k - \Phi_k^A (\Phi_k^A)^T) Y \right\|_F = \sqrt{\sum_{i=k+1}^r (\lambda_i^A)^2},$$

where λ_i^A is the i th singular value of X^A . When $r^A \leq k$, the SVD or the GramSchmidt process could be used to obtain r^A orthonormal bases that span \mathcal{S}_r^A . Choose any additional $k - r^A$ vectors to form an $n \times k$ matrix $\Phi_k^A \in \mathcal{V}_{n \times k}$, (5.17) becomes $E_k^A = 0$. Comparing E_k with E_k^A , we have the following lemma.

LEMMA 5.4. *Let X and X^A be the matrices for solution snapshots and weighted solution snapshots. E_k and E_k^A are projection errors respectively given by (4.4) (5.17). Then, $E_k \geq E_k^A$.*

Proof. When $r^A \leq k$, the conclusion holds trivially. We consider the case for $r^A > k$. For each weighing coefficient a_i in X^A , we have $0 \leq a_i \leq 1$. It follows that

$$(5.18) \quad \begin{aligned} \left\| (I_k - \Phi_k \Phi_k^T) X \right\|_F &= \left\| (I_k - \Phi_k \Phi_k^T) u_1, \dots, (I_k - \Phi_k \Phi_k^T) u_p \right\|_F \\ &\geq \left\| (I_k - \Phi_k \Phi_k^T) a_1 u_1, \dots, (I_k - \Phi_k \Phi_k^T) a_p u_p \right\|_F \\ &= \left\| (I_k - \Phi_k \Phi_k^T) X^A \right\|_F \\ &\geq \left\| (I_k - \Phi_k^A (\Phi_k^A)^T) X^A \right\|_F. \end{aligned}$$

The last inequity holds because Φ_k^A provides a least Frobenius norm for the difference of matrix X^A and its projection onto a k -dimensional subspace. Using the definition of E_k and E_k^A , one obtains $E_k \geq E_k^A$. Especially, $E_k = E_k^A$ holds if and only if for any i , $a_i = 1$. In this case, the ARM degenerates to the GRM. \square

COROLLARY 5.5. *Let X and X^L be the matrices for solution snapshots and local solution snapshots. E_k and E_k^L are projection errors. Then, $E_k > E_k^L$.*

Proof. We construct a $n \times p$ matrix $X' = [b_1 u_1, \dots, b_p u_p]$. Let $b_i = 1$ when $i \in \mathcal{D}^L$ and $b_i = 0$ otherwise. Essentially, X' is an extension of X^L with some 0 column vectors. SVD of X' and X^L gives the same POD basis matrix Φ_k^L and

singular values λ_i^L . Therefore, the projection error in Frobenius norm, E_k^L , is given by $\|(I_k - \Phi_k^L(\Phi_k^L)^T)X'\|_F$. Since $b_i = 0$ for some i , by lemma 5.4, it follows that

$$(5.19) \quad \|(I_k - \Phi_k \Phi_k^T)X\|_F > \|(I_k - \Phi_k^L(\Phi_k^L)^T)X'\|_F.$$

The above equation means $E_k > E_k^L$, i.e., the projection error of the LRM is smaller than the error from the GRM. \square

Lemma 5.4 and corollary 5.5 compare projection error of the same data ensemble $\{u_i\}_{i=1}^p$, and suggests that E_k^A and E_k^L is usually smaller than E_k . Furthermore, for a specified parameter μ_* , if the projection \tilde{u}_r of u_* has a form of (5.15), the SVD truncation error e_o^A of the ARM is bounded by a constant times E_k^A ,

$$(5.20) \quad \begin{aligned} \|e_o^A\| &= \|\tilde{u}_r^A - \tilde{u}_k^A\| = \left\| \sum_{i=1}^p (1 + \eta_i) a_i u_i - (1 + \eta_i) a_i (\Phi_k^A(\Phi_k^A)^T) u_i \right\| \\ &\leq \sum_{i=1}^p \left\| (I - \Phi_k^A(\Phi_k^A)^T) (1 + \eta_i) a_i u_i \right\| \leq \max_i (1 + \eta_i) \sum_{i=1}^p \left\| (I - \Phi_k^A(\Phi_k^A)^T) a_i u_i \right\| \\ &\leq (1 + \epsilon_\eta) E_k^A. \end{aligned}$$

The error bound of e_o of the GRM has the similar property

$$(5.21) \quad \begin{aligned} \|e_o\| &= \|\tilde{u}_r - \tilde{u}_k\| = \left\| \sum_{i=1}^p (1 + \eta_i) a_i u_i - (1 + \eta_i) \eta_i a_i (\Phi_k \Phi_k^T) u_i \right\| \\ &\leq \sum_{i=1}^p \left\| (I - \Phi_k \Phi_k^T) (1 + \eta_i) a_i u_i \right\| \leq \max_i (1 + \eta_i) \|a_i\| \sum_{i=1}^p \left\| (I - \Phi_k \Phi_k^T) u_i \right\| \\ &\leq (1 + \epsilon_\eta) E_k \end{aligned}$$

Combined (5.20) with (5.21), and using lemma (5.4), we conclude that the upper error bound of e_o^A is smaller than e_o , provided that $\tilde{u}_r^A = \Phi_r \Phi_r^T u_*$.

We next consider the projection error of u_* onto a Lagrange subspace spanned by solution snapshots. Since GRM uses all the solution snapshots, while ARM and LRM only use partial snapshots, it immediately follows that $\|e_r\| \leq \|e_r^A\|$, and $\|e_r\| < \|e_r^L\|$. More specifically, suppose the output u is a smooth function of μ , using Lagrange interpolation, u_* could be expended in terms of $\{u_i\}_{i=1}^p$. The first few interpolation coefficients could be matched. The remainders can be expressed by a higher order term. Roughly speaking, we have $\|e_r\| < \min_{i=1}^s c_i(\mu_*) \delta(\mu_*, i)^i$, where $c_i(\mu_*)$ denotes the norm of i th order derivative of u at μ_* , $\delta(\mu_*, i)$ denotes the norm distance from μ_* to the its nearest q neighbors. Let m be the dimension of μ , then $q = \binom{m+i}{i}$.

s denotes the largest integer that satisfies $s \leq \binom{m+p}{p}$. As more snapshots is counted to form the snapshot matrix, s and $\delta(\mu_*, s)$ increase simultaneously. Therefore, only local snapshots contribute significantly to reduce e_r . The above analysis also applies for the APM and LRM. For this reason, $\|e_r^A\|$ could be very near to $\|e_r\|$ as long as the weighting coefficients for many local snapshots near μ_* are nonzero.

Replacing u_i by g_i , we can use the same procedure to compute the collateral reduced basis for nonlinear snapshots by SVD for the following collateral weighted snapshot matrix,

$$(5.22) \quad Y = [a_1 g_1, \dots, a_p g_p],$$

and then use the ARM for the reduced chord iteration.

5.3. Numerical Example. In this subsection, the adaptive reduced model is applied to an elliptic PDE (from [10] and [5]),

$$(5.23) \quad -\nabla^2 u(x, y) + \frac{\mu_1}{\mu_2}(\mathrm{e}^{\mu_2 u} - 1) = 100 \cos(2\pi x) \cos(2\pi y),$$

with homogeneous Dirichlet boundary conditions,

$$(5.24) \quad u(0, y) = u(1, y) = u(x, 0) = u(x, 1) = 0.$$

The spatial variables $(x, y) \in \Omega = [0, 1]^2$ and the parameters satisfy $\mu = (\mu_1, \mu_2) \in \mathcal{D} = [0.01, 10]^2 \subset \mathbb{R}^2$. The “real” solution is solved by Newton iteration resulting from a finite difference discretization. The spatial grid points (x_i, y_j) are equally spaced in Ω for $i, j = 1, \dots, 50$. The full dimension for the state variable u is then $n = 2500$.

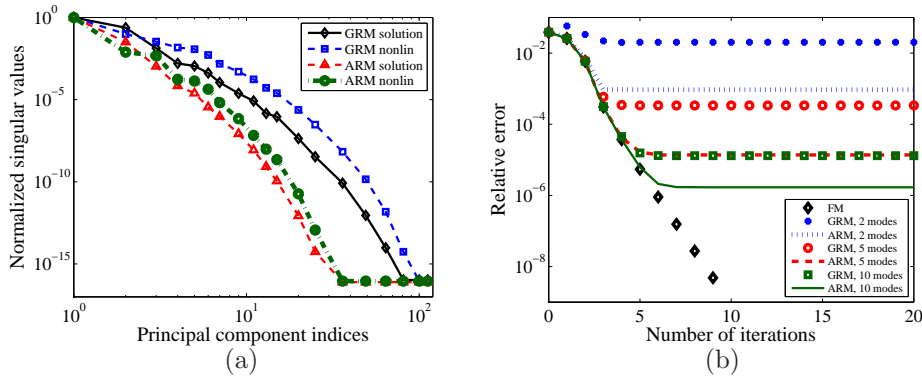


FIGURE 5.1. (Color online.) Simulation results for equation (5.23). (a) Normalized singular values of the information matrices of solution snapshots Y defined by (5.16) and of nonlinear snapshots Y' defined by (5.22). The singular values of Y and Y' in adaptive reduced model (ARM) decrease faster than the corresponding values in global reduced model (GRM). Singular values of Y decrease faster than the singular values of Y' . (b) The relative error for chord iteration and its reduced model. The full model (FM) is computed by 50×50 grid points. For the reduced model, the POD-DEIM approach is used. We set the subspace dimension for the nonlinear term $s(u, \mu)$ twice as the subspace dimension for the solution u to balance the POD error and the error from DEIM approximation. For both GRM and ARM, solution subspaces are spanned by 2, 5, and 10 modes respectively, and the subspaces for nonlinear term are spanned by 4, 10, 20 accordingly. The relative error is defined as $\|u(\mu) - \hat{u}(\mu)\|_2 / \|u(\mu)\|_2$.

Figures 5.1(a) shows the normalized singular values for the solution snapshots of (5.23) and nonlinear snapshots $s(u, \mu) = \mu_1/\mu_2(\exp(\mu_2 u) - 1)$ of the uniformly selected 121 input parameters, for the global reduced model (GRM) and the adaptive reduced model (ARM) discussed in section 5.2. All the singular values are normalized by the one corresponds to the first singular mode. Compared with GRM, the singular values in ARM has faster decreasing rate, which means in order to obtain the same level of accuracy, ARM needs fewer modes to represent the original system. Figure 5.1(b) shows that the ARM formed by POD-DEIM reduced system can accurately reproduce the solution of the full-order system of dimension 2500 with relative error $\mathcal{O}(10^{-3})$ by 2 modes to approximate solution snapshots, with relative error $\mathcal{O}(10^{-5})$ by 5 modes and with relative error $\mathcal{O}(10^{-6})$ by 10 modes. Since the normalized singular values of the nonlinear snapshots decrease slower than the values of solution snapshots, we set the dimension of collateral subspace twice as the dimension of the solution subspace. As expected, APM has much higher accuracy than GRM for the same dimension.

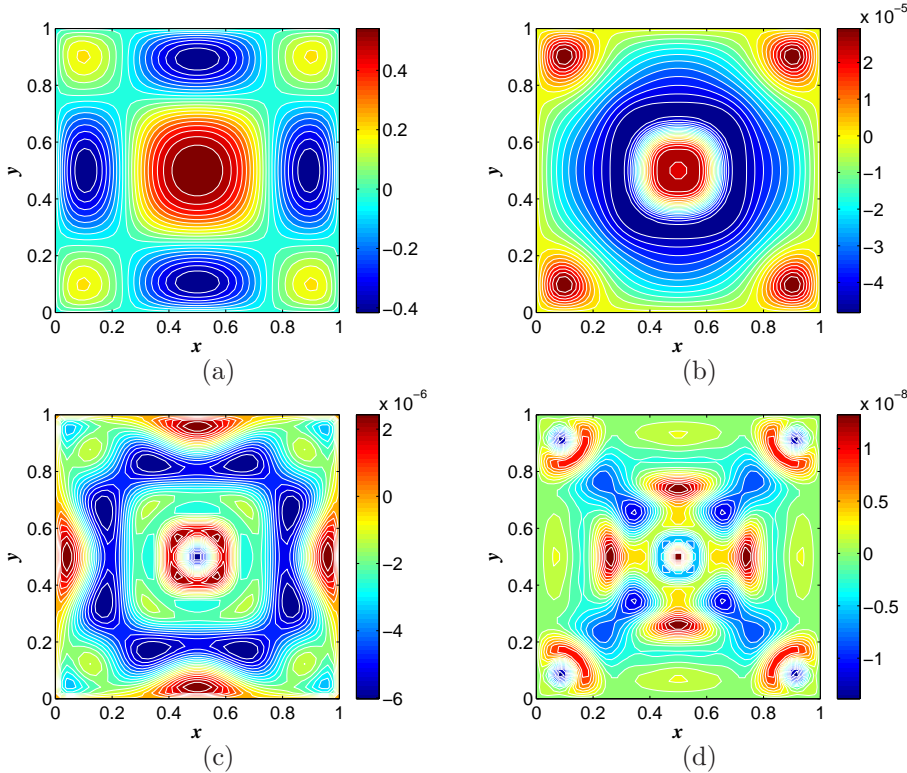


FIGURE 5.2. (Color online.) Simulation results for the elliptic equation (5.23) with $\mu = (\mu_1, \mu_2) = (4.5, 8.5)$. (a) The solution snapshot computed by the full model with $\text{dim} = 2500$. (b) Relative errors at the grid points with the solution from the POD-DEIM reduced system for solution $\text{dim} = 2$ with nonlinear term $\text{dim} = 4$. (c) Relative errors for solution $\text{dim} = 5$ with nonlinear term $\text{dim} = 10$. (d) Relative errors for solution $\text{dim} = 10$ with nonlinear term $\text{dim} = 20$. The reduced model formed by ARM could obtain the same accuracy level in a lower dimensional subspace.

These errors are averaged over a set of 100 parameters μ that were not used to obtain the sample snapshots. This suggests that the POD-DEIM reduced system can give a good approximation to the original system with any value of parameter $\mu \in \mathcal{D}$. Figure 5.2 (a) shows the snapshot corresponding to the input parameters $\mu_1 = 4.5$, and $\mu_2 = 8.5$. Figures 5.2(b)-5.2(d) respectively show the relative errors at the grid points from the solution of the POD-DEIM reduced system with solution dimension as 2, 5, and 10, respectively.

6. Nonlinear Parabolic PDEs. In this section, we extend our adaptive model reduction approach to treat nonlinear parabolic PDEs. We first briefly review the reduced models formed by Galerkin projection and DEIM and apply the adaptive reduced basis approach. Then, we discuss numerical results obtained with the proposed method.

6.1. Methodology. The description of many dynamical systems involves solving partial differential equations (PDEs) with first order time-derivative terms. Let $I = [0, T]$ denotes the time domain. After spatial discretization (for example, using finite difference or finite element methods), the projection on \mathbb{R}^n is given by an ordinary differential equations (ODE)

$$(6.1) \quad \dot{u} = f(t, \mu, u),$$

and its initial condition $u(0, \mu) = u_0$. Here, $u : I \times \mathcal{D} \rightarrow \mathbb{R}^n$ and the discretized vector field $f : I \times \mathbb{R}^m \times \mathbb{R}^n \rightarrow \mathbb{R}^n$ becomes an algebraic operator. By definition, $u(t, \mu)$ is a flow which gives an orbit in \mathbb{R}^n as t varies over I for a fixed initial condition u_0 and a fixed input parameter $\mu \in \mathcal{D}$. The orbit contains a sequence of states (or state vectors) that follow from u_0 .

For a k -dimensional linear subspace \mathcal{S} in \mathbb{R}^n , there exists an $n \times k$ orthonormal matrix $\Phi = (\phi_1, \dots, \phi_k)$, whose columns form a complete basis vectors of \mathcal{S} . Any state $u \in \mathbb{R}^n$ can be projected onto \mathcal{S} by a linear projection mapping. In the subspace coordinate system, the projected state is given by $\Phi^T u \in \mathbb{R}^k$, where the superscript T denotes matrix transpose. Let $P := \Phi \Phi^T$ denotes the projection matrix in \mathbb{R}^n . Then, the same projection in the original coordinate system is represented by $\tilde{u}(t, \mu) := P u(t, \mu) \in \mathbb{R}^n$.

Let $\Phi^T f(t, \mu, \Phi z)$ denote a reduced vector field formed by the Galerkin projection. The corresponding reduced model for $z(t) \in \mathbb{R}^k$ is

$$(6.2) \quad \dot{z} = \Phi^T f(t, \mu, \Phi z).$$

The initial condition in subspace coordinates can be set as $z_0 = \Phi^T x_0$. An approximating solution in the original coordinate system $\hat{x}(t) = \Phi z(t) \in \mathbb{R}^n$ is equivalent to the solution of the following ODE

$$(6.3) \quad \dot{\hat{u}} = P f(t, \mu, \hat{u}),$$

with $\hat{u}_0 = P u_0$ as the initial condition. Usually, unless $f(t, \mu, x)$ is a linear function, the standard Galerkin projection 6.2 may not be able to obtain real speedups for online computation. The DEIM could be used here if we replay μ by (t, μ) in (4.9), and all the others remains the same.

In the offline computation, for each input parameter μ_i the solution trajectory gives a snapshot matrix $X_i = [u(t_1, \mu_i), \dots, u(t_T, \mu_i)]$. Using standard SVD, we have $X_i = V_i \Lambda_i W_i^T$, where $V_i = [v_1(\mu_i), \dots, v_{r_i}(\mu_i)]$ is a set of orthonormal bases, $\Lambda_i = \text{diag}\{\lambda_1(\mu_i), \dots, \lambda_{r_i}(\mu_i)\}$ contains the corresponding eigenvalues. The POD bases Φ_i is given by the first k_i columns of V_i . Correspondingly the Λ'_i is defined as the first $k_i \times k_i$ block of Λ_i . Then Φ_i minimize the truncation error of X_i and its projection onto the column space of Φ_i , which is given by $E_i = \|(I - \Phi_i \Phi_i^T) X_i\|_F$.

We shall use adaptive reduced bases to form a reduced model. As an analogy of (5.16), the weighted snapshot matrix for the ODE, can be defined by

$$(6.4) \quad X^A = [a_1 X_1, \dots, a_p X_p],$$

where $\{a_i\}_{i=1}^p$ are the weighting coefficients for the new parameter μ_* , corresponding to (??). This is slight different than the coefficient of algebraic equations in the previous section, where a_i is computed based on a reference point $\mu_\#$. Usually, time integration for a parabolic equation is much more expensive than a few iterations based on the reduced chord method. On the other hand, the norm error grows exponentially for a parabolic equation, and decreasing the projection error is crucial to limit the total error. Therefore, computing the adaptive bases is carried out in the online stage for a parabolic equation and in the offline stage for an elliptic equation.

Direct SVD for X^A could obtain reduced bases, but it is not optimal. First, X^A needs a large memory to record, especially when the trajectories show fast variation over a long time domain. Suppose we pick T snapshots from each trajectory, then

the total size of X is $n \times pT$. Secondly, it could be very time consuming for SVD. To treat this issue, an information matrix is set as

$$(6.5) \quad \tilde{X}^A = [a_1 \Phi_1 \Lambda'_1, \dots, a_p \Phi_p \Lambda'_p].$$

Suppose each Φ_k is a $n \times k$ matrix, then the size of \tilde{X}^A is $n \times pk$. The adaptive reduced bases can be computed by the SVD for \tilde{X}^A .

LEMMA 6.1. *Let Φ minimize the truncation error of \tilde{X}^A and its projection onto the column space of Φ , which is given by $E_0 = \|(I - \Phi \Phi^T) \tilde{X}^A\|_F$. Then the projection error for the original weighted snapshot matrix X (6.4) is bounded by*

$$(6.6) \quad \|(I - \Phi \Phi^T) X\|_F \leq E_0 + \sqrt{\sum_{i=1}^p a_i^2 E_i^2}.$$

Proof. Since non-truncated SVD gives $X_i = V_i \Lambda_i W_i^T$, by the definition of X , we have $X = [a_1 V_1 \Lambda_1 W_1^T, \dots, a_p V_p \Lambda_p W_p^T]$. We construct a new matrix

$$\tilde{X} := [a_1 V_1 \tilde{\Lambda}_1 W_1, \dots, a_p V_p \tilde{\Lambda}_p W_p^T],$$

where $\tilde{\Lambda}_i$ is a $n \times n$ matrix, but only contains the first k_i nonzero singular values of Λ_i , i.e., $\Lambda_i = \text{diag}\{\lambda_1(\mu_i), \dots, \lambda_{k_i}(\mu_i), 0, \dots, 0\}$. Since W_i are orthonormal,

$$(6.7) \quad (X - \tilde{X})(X - \tilde{X})^T = \sum_{i=1}^p a_i^2 V_i (\Lambda_i - \tilde{\Lambda}_i)^2 V_i^T.$$

It follows that

$$(6.8) \quad \begin{aligned} \|X - \tilde{X}\|_F^2 &= \text{tr} \left((X - \tilde{X})(X - \tilde{X})^T \right) = \sum_{i=1}^p \text{tr}(a_i^2 V_i (\Lambda_i - \tilde{\Lambda}_i)^2 V_i^T) \\ &= \sum_{i=1}^p a_i^2 \text{tr}((\Lambda_i - \tilde{\Lambda}_i)^2) = \sum_{i=1}^p a_i^2 E_i^2 \end{aligned}$$

The last equity holds because $E_i = \|(I - \Phi_i \Phi_i^T) X_i\|_F = \sqrt{\sum_{j=k_i+1}^{r_i} \lambda_j^2}$. On the other hand,

$$(6.9) \quad \begin{aligned} \|(I - \Phi \Phi^T) \tilde{X}\|_F &= \|(I - \Phi \Phi^T)[a_1 V_1 \tilde{\Lambda}'_1, \dots, a_p V_p \tilde{\Lambda}'_p] \text{diag}\{W_1^T, \dots, W_p^T\}\|_F \\ &= \|(I - \Phi \Phi^T)[a_1 V_1 \tilde{\Lambda}'_1, \dots, a_p V_p \tilde{\Lambda}'_p]\|_F = \|(I - \Phi \Phi^T)[a_1 \Phi_1 \Lambda'_1, \dots, a_p \Phi_p \Lambda'_p]\|_F \\ &= \|(I - \Phi \Phi^T) \tilde{X}^A\|_F = E_0 \end{aligned}$$

Using (6.8) and (6.9), and combining the following inequality,

$$(6.10) \quad \begin{aligned} \|(I - \Phi \Phi^T) X\|_F &\leq \|(I - \Phi \Phi^T) \tilde{X}\|_F + \|(I - \Phi \Phi^T)(X - \tilde{X})\|_F \\ &\leq \|(I - \Phi \Phi^T) \tilde{X}\|_F + \|X - \tilde{X}\|_F \end{aligned}$$

(6.6) is obtained. \square

Similarly the collateral information matrix for the nonlinear snapshots shares the similar expression, i.e.,

$$(6.11) \quad Y = [a_1 \Psi_1 \Sigma_1, \dots, a_p \Psi_p \Sigma_p],$$

where Ψ_i and Σ_i are computed by truncated SVD for the nonlinear snapshots on the trajectory $u(\mu_i)$. Having two sets of basis vectors, the POD-DEIM approach could be used to form a reduced model.

Suppose as the weighting interpolation coefficients a_i s are continuous functions of μ for each new online computation. Then $\tilde{X}^A(\mu)$ could be considered as a continuous matrix-valued function of parameter μ_* . The truncated SVD is a continuous map from \tilde{X}^A to Φ . It follows that the mapping $\mathcal{S} : \mu \mapsto \mathcal{S}(\mu)$ is a continuous function from parameter space to Grassmann manifold. Finally, the solution of a reduced equation $\hat{u}(t, \mu)$, formed by POD-Galerkin approach or POD-DEIM approach, is a smooth function of μ .

6.2. Numerical Example. The proposed algorithm is illustrated in this subsection by testing it to solve the one dimensional Burgers equation, which focuses on demonstrating the capability of adaptive reduced model to deliver accurate results.

Let $u = u(t, x)$. Consider the one-dimensional Burgers equation with constant diffusion coefficient ν ,

$$(6.12) \quad \frac{\partial u}{\partial t} = -u \frac{\partial u}{\partial x} + \nu \frac{\partial^2 u}{\partial x^2},$$

on space $x \in [0, 1]$. Without loss of generality, periodic boundary conditions are applied, with $u(t, 0) = u(t, 1)$, and $u_x(t, 0) = u_x(t, 1)$. The initial condition is provided by a Gaussian function $u(0, x) = \exp(-12.5(x - 1/3)^2)$.

The fully resolved model is obtained through a high resolution finite difference simulation with spatial discretization by $n = 1000$ equally spaced grid points. The advection term is discretized by the first-order upwind difference scheme with the forward Euler method for time integration while the diffusion term is discretized by the second-order central difference scheme with the Crank-Nicolson method for time integration.

In the simulation we set the diffusion coefficients ν from 0.001 to 0.01 with equally spaced intervals 0.001. For each trajectory, the first 100 modes with singular values of solution snapshots and the first 150 modes with singular values of nonlinear snapshots are restored. Figures 6.1 shows the normalized singular values of the information matrices Y and Y' . If all a_i s equal 1, this degenerates to the global reduced model (GRM) and if a_i is formed by the interpolation scheme mentioned above, it corresponds to the adaptive reduced model (ARM). The normalization is taken by dividing the largest singular values. The singular values in ARM have faster decreasing rate, which means in order to obtain the same level of accuracy, ARM needs less modes represent the original system. There are kinks for both GRM and ARM when the principle component indices are greater than 100 for Y and 150 for Y' , this is due to the truncation from the SVD of the original trajectory for each old parameter.

Since one-dimensional Burgers equation has a positive velocity, a wave will propagate to the right with the higher velocities overcoming the lower velocities and creating steep gradients. This steepening continues until a balance with the dissipation is reached, as shown by the velocity profile at $t = 1$ in Figure 6.2(a). Since states of Burgers equation show a high variability with time evolution, compared with an

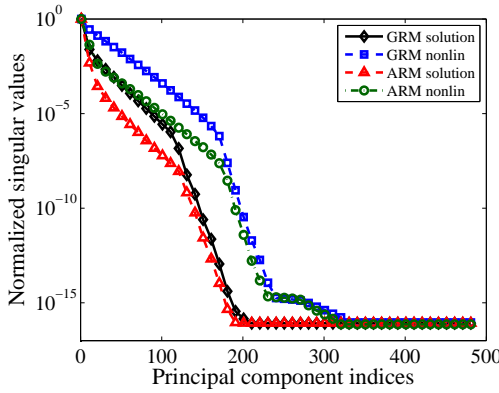


FIGURE 6.1. (Color online.) Normalized singular values of the information matrices of solution snapshots Y and of nonlinear snapshots Y' from (6.12). ARM has faster decreasing rate compared with GRM.

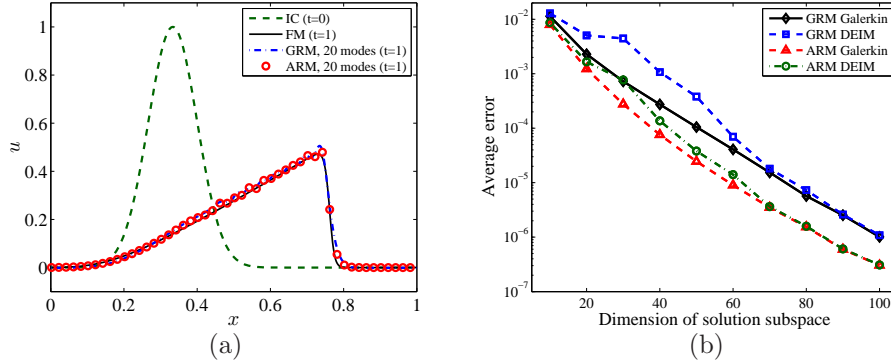


FIGURE 6.2. (Color online.) Simulation results for one-dimensional Burgers equation (6.12) with fixed space domain $[0, 1]$. (a) The velocity profiles at $t = 0$ and $t = 1$ with constant diffusion coefficient $\nu = 1.5 \times 10^{-3}$. 1000 grid points are used to obtain the full model (FM). For both global reduced model (GRM) and adaptive reduced model (ARM), the solution is obtained from the POD-DEIM reduced system for solution $\text{dim} = 20$ with nonlinear term $\text{dim} = 40$. (b) Error plot for ARM and GRM obtained by the Galerkin projection and DEIM. Plot of the maximal difference between the benchmark solution $u(t)$ and the approximating solution $\hat{u}(t)$, $\|e\|_\infty = \sup\{\|u_*(t) - \hat{u}(t)\|_\infty : t \in [0, 0.1]\}$. One on hand, reduced model formed by DEIM could be a good approximation for Galerkin, especially when the dimension increases. One the other hand, for the same dimension, ARM could always obtain higher accuracy compared with GRM.

elliptic equation more modes are needed in order to present the whole solution trajectory with high accuracy. Figure 6.2(b) shows the average norm 2 error for both ARM and GRM for 10 new parameters where the reduced models are formed by standard Galerkin projection and DEIM. For the DEIM case, the dimension for nonlinear snapshots approximation is 1.5 times of dimension of the solution snapshots. It is noticed that GRM always has higher error than ARM when they share the same dimension.

7. Conclusion. In this paper, we provide a new method to form adaptive reduced bases for model reduction of large-scale parameterized PDEs. The method could be applied to both elliptic and parabolic PDEs based on proper orthogonal decomposition (POD) and discrete empirical interpolation method (DEIM). For elliptic PDEs, the basis vectors of solution subspace and nonlinear term subspace are

respectively computed by singular value decomposition (SVD) of the information matrices, whose columns are defined as the weighted solution snapshots and nonlinear snapshots in the original equation. For parabolic PDEs, the information matrices for solution subspace and nonlinear term subspace are respectively computed from a set of empirical eigenfunctions times the corresponding empirical eigenvalues from the precomputed trajectories. We provided an analytic proof to show that the proposed method could decrease truncation error by SVD. Moreover, we demonstrated that the reduced equation corresponding to adaptive information matrices gives much higher accuracy than the global reduced model with the same subspace dimension in an elliptic PDE and a one-dimensional Burgers equation.

REFERENCES

- [1] M. AMABILI, A. SARKAR, AND M. P. PAIDOUSSIS, *Reduced-order models for nonlinear vibrations of cylindrical shells via the proper orthogonal decomposition method*, Journal of Fluids and Structures, 18 (2003), pp. 227–250.
- [2] D. AMSALLEM AND C. FARHAT, *A method for interpolating on manifolds structural dynamics reduced-order models*, Int. J. Num. Methods in Eng., 80 (2009), pp. 1241–1257.
- [3] M. BARRAULT, Y. MADAY, N. C. NGUYEN, AND A. T. PATERA, *An ‘empirical interpolation’ method: Application to efficient reduced-basis discretization of partial differential equations*, C. R. Acad. Sci. Paris, Ser. I, 339 (2004), pp. 667–672.
- [4] K. CARLBERG, C. BOU-MOSLEH, AND C. FARHAT, *Efficient non-linear model reduction via a least-squares petrov-galerkin projection and compressive tensor approximations*, Int. J. Num. Methods in Eng., 86 (2011), pp. 155–181.
- [5] S. CHATURANTABUT AND D. C. SORENSEN, *Nonlinear model reduction via discrete empirical interpolation*, SIAM J. Sci. Comput., 32 (2010), pp. 2737–2764.
- [6] C. F. D. AMSALLEM, M. J. ZAHR, *Nonlinear model order reduction based on local reduced-order bases*, in press in the International Journal for Numerical Methods in Engineering, (2012). available online.
- [7] M. DIHLMANN, M. DROHMAN, AND B. HAASDONK, *Model reduction of parametrized evolution problems using the reduced basis method with adaptive time partitioning*, Technical Report 2011-13, Stuttgart Research Centre for Simulation Technology, Stuttgart, Germany, May 2011.
- [8] J. L. EFTANG, A. T. PATERA, AND E. M. R. NQUIST, *An “hp” certified reduced basis method for parametrized elliptic partial differential equations*, SIAM J. Sci. Comput., 32 (2010), pp. 3170–3200.
- [9] M. GRAHAM AND I. KEVREKIDIS, *Alternative approaches to the Karhunen-Loève decomposition for model reduction and data analysis*, Computers and Chemical Engineering, 20 (1996), pp. 495–506.
- [10] M. A. GREPL, Y. MADAY, N. C. NGUYEN, AND A. T. PATERA, *Efficient reduced-basis treatment of nonaffine and nonlinear partial differential equations*, M2AN Math. Model. Numer. Anal., 41 (2007), pp. 575–605.
- [11] P. HOLMES, J. LUMLEY, AND G. BERKOOZ, *Turbulence, Coherent Structures, Dynamical Systems and Symmetry*, Cambridge Univ. Press, Cambridge, UK, 1998.
- [12] C. KELLEY, *Iterative methods for linear and nonlinear equations*, SIAM publication, Philadelphia, 1995.
- [13] K. KUNISCH AND S. VOLKWEIN, *Galerkin proper orthogonal decomposition methods for a general equation in fluid dynamics*, SIAM J. Numer. Anal., 40 (2002), pp. 492–515.
- [14] T. LIEU AND M. LESOINNE, *Parameter adaptation of reduced order models for three-dimensional flutter analysis*, 2004.
- [15] L. PENG AND K. MOHSENI, *An online manifold learning approach for model reduction of dynamical systems*, submitted to SIAM J. Numer. Anal., (2012). Also <http://arxiv.org/abs/1210.2975>.
- [16] T. A. PORSCHING, *Estimation of the error in the reduced basis method solution of nonlinear equations*, Mathematics of Computation, 45 (1985), pp. 487–496.
- [17] M. RATHINAM AND L. R. PETZOLD, *Dynamic iteration using reduced order models: A method for simulation of large scale modular systems*, SIAM J. Numer. Anal., 40 (2002), pp. 1446–1474.
- [18] ———, *A new look at proper orthogonal decomposition*, SIAM J. Numer. Anal., 41 (2003),

pp. 1893–1925.

- [19] C. W. ROWLEY, T. COLONIUS, AND R. M. MURRA, *Model reduction for compressible flows using POD and Galerkin projection*, Physica D, 189 (2004), pp. 115–129.
- [20] Y. SAAD, *Iterative methods for sparse linear systems (2nd edn)*, SIAM publication, Philadelphia, 2003.
- [21] R. SCHMIT AND M. GLAUSER, *Improvements in low dimensional tools for flow-structure interaction problems: using global pod*, 2004.

NONLINEAR MODEL REDUCTION VIA ADAPTIVE REDUCED BASES*

LIQIAN PENG[†] AND KAMRAN MOHSENI[‡]

Abstract. A new approach to model reduction of parameterized partial differential equations (PDEs) based on the concept of adaptive reduced bases is introduced. The presented approach is particularly suited for large-scale nonlinear systems characterized by parameter variations. Instead of approximating the solution of interest in a subspace spanned by global basis vectors, the proposed method approximates this solution in a lower-dimensional subspace generated by weighted snapshots, and each weighting coefficient is a function of the input parameter. Compared with global proper orthogonal decomposition, a more accurate approximating solution could be solved in a subspace with much fewer dimensions by the proposed method. Moreover, the corresponding reduced model can be formed by the discrete empirical interpolation method. Thus, the proposed method for nonlinear model order reduction is computationally efficient. The potential of the method for achieving large speedups while maintaining good accuracy is demonstrated for both elliptic and parabolic PDEs in two numerical examples.

1. Introduction. Due to computing speed barriers, in many engineering applications, direct numerical simulations are so computationally intensive that they either cannot be performed as often as needed or are more often performed in special circumstances than routinely. For this reason, during the past several decades, many efforts have been put forward to develop reduced models on time-critical operations such as electrical power grids [?], structural dynamics [?], chemical reaction systems [?], and CFD-based modelling and control [?, ?] to list a few. The core of model reduction is based on the fact that although the state of a complex system is in general represented by a large dimensional space, the linear subspace spanned by solution snapshots actually has a much lower dimension. To this effect, the proper orthogonal decomposition (POD) [?] or reduced basis methods [?] are developed to generate lower dimensional surrogates for the original large-scale complex problems. Although POD always looks for linear subspace instead of its curved submanifold, it is computationally tractable and able to capture the dominant patterns in a nonlinear system.

Compared with online dimensionality reduction methodology [?, ?], the offline-online splitting methodology is more often used in the real-time or many-query contexts to achieve minimal marginal cost per input-output evaluation. In the offline stage, the original problem corresponding to some sampled input parameters is solved to obtain some solution snapshots. For the online computation, a linear subspace for new input-output evaluation is constructed. To the best of our knowledge, there are at least three methods have been considered in the context of the reduced basis method: the global POD method, the local POD method and the adaptive POD method. The global POD method approximates the solution of interest in a subspace spanned by global basis vectors [?]. All the snapshots contribute equally to form the subspace. This method is straightforward for application, however, in order to obtain a high accuracy, a subspace with relatively high dimension should be used to construct the reduced model, especially when there exist many solution modes for

*This research was supported by the Office of Naval Research.

[†]Department of Mechanical and Aerospace Engineering, and Institute for Networked Autonomous Systems, University of Florida, Gainesville, FL, 32611-6250 (liqianpeng@ufl.edu).

[‡]Department of Mechanical and Aerospace Engineering, Department of Electrical and Computer Engineering, and Institute for Networked Autonomous Systems, University of Florida, Gainesville, FL, 32611-6250 (mohseni@ufl.edu).

the whole interested domain. Thus, global POD method inevitably keeps some redundant dimensions in the online computation and leads to long online simulation times. In order to form reduced model with significant lower dimension, local POD methods generate local reduced models by project the original equation onto a set of local reduced bases which corresponds to partial pre-computed snapshots. These snapshots are clustered through time domain partition [?], space domain partition [?] or parameter domain partition [?]. Local reduced models need less extra dimensions to present an approximating solution, but its solution cannot obtain a high order accuracy unless enough local data is given. The other method use global data, but form an adaptive reduced basis through an interpolation scheme. It could be directly computed by the subspace angle interpolation approach [?] or the interpolation in the tangent space of Grassmann manifold [?]. Although these adaptive POD interpolation methods could construct new a subspace for each new parameter, the dimension of all the pre-computed subspaces and the new subspace are fixed to a same value. Thus, there is no flexibility to change the new subspace dimension in order to balance the accuracy and the approximating error of reduced models. Moreover, the subspace interpolation process inevitably introduce some numerical error and the corresponding error bound is difficult to estimate.

Once a subspace is obtained, reduced models are typically constructed by Galerkin projection. However, the Galerkin approach is limited to the problems of linear equation or low-order polynomial nonlinearities. When a general nonlinearity is present, the cost to evaluate the projected nonlinear function still depends on the dimension of the original system, resulting in simulation times that hardly improve over the original system. To this effect, the empirical interpolation method [?, ?], and its variant, discrete empirical interpolation (DEIM) [?] were developed to approximate the original system by constructing surrogates for the nonlinear terms of the original equation using a data fitting approach that employs their values at a few indices and a set of pre-determined shape functions.

In this paper, we provide a new method to form an adaptive reduced model for the parameter variation. The dimension of the reduced model could be adaptively chosen to obtain a certain level of accuracy. The basis vectors are directly computed by the singular value decomposition (SVD) of a weighted snapshot matrix, whose columns are defined as the pre-computed snapshots multiplies weighting coefficients, which are similar to the coefficients for direction interpolation of the solution snapshots in the parameter space. When a compact interpolation scheme is used, the subspace it generates is similar to the one from a local POD method. When all the coefficients in the information matrix are set equally, this method degenerates to a global POD method. When a noncompact scheme is used, such as radial basis function or inverse distance weighting, the subspace behaves similar to local POD when the dimension is low and similar to global POD when the dimension is high. We demonstrate that reduced equation corresponding to this subspace gives much higher accuracy than the global reduced model with the same subspace dimension. Furthermore, the adaptive reduced model could be formed by the POD-DEIM approach, and therefore it is very efficient.

The remainder of this article is organized as follows. In section 2 and 3, an overview of model reduction for parameterized PDEs and a general error analysis are presented. Section 4 briefly reviews the classical POD-Galerkin method and its variant POD-DEIM method. Then a general method for elliptic PDEs is discussed in section 5. After introduce the chord method, we apply the classical POD method

for model reduction. Then adaptive reduced bases is proposed in order to use fewer modes to approximate the original system. Section 6 extends the adaptive reduced model to parabolic PDEs. Finally, conclusions are offered in section 7.

2. Formulation of Parameterized PDEs. We consider both parabolic PDEs and elliptic PDEs in this section. By discretization (for example, using finite difference or finite element methods), an elliptic parameterized PDE for variable $u \in \mathbb{R}^n$ with input parameter $\mu \in \mathbb{R}^m$ can be expressed as an algebraic equation

$$(2.1) \quad f(\mu, u) = 0,$$

where $f : \mathcal{D} \times \mathcal{R} \rightarrow \mathbb{R}^n$ is a smooth function for $\mathcal{D} \subset \mathbb{R}^m$ and $\mathcal{R} \subset \mathbb{R}^n$. For any fixed input parameter $\mu \in \mathcal{D}$, we seek a solution $u = u(\mu) \in \mathcal{R}$, such that $f(\mu, u) = 0$ could be satisfied.

Parabolic PDEs are often used to describe dynamical systems with time dependent solutions. Let $\mathcal{I} = [0, T]$ denote the time domain and \mathcal{D} denote the parameter domain. By spatial discretization, the original parabolic PDE becomes an ordinary differential equation (ODE)

$$(2.2) \quad \dot{u} = f(t, \mu, u),$$

with an initial condition $u(0, \mu) = u_0$, where $f : \mathcal{I} \times \mathcal{D} \times \mathcal{R} \rightarrow \mathbb{R}^n$ denotes the discretized vector field. For any fixed $t \in \mathcal{I}$ and $\mu \in \mathcal{D}$, the state variable $u = u(t, \mu) \in \mathcal{R} \subset \mathbb{R}^n$ satisfies (2.2). By definition, $u(t, \mu)$ is a flow which gives an orbit in \mathbb{R}^n as t varies over \mathcal{I} for a fixed initial condition u_0 and a fixed input parameter $\mu \in \mathcal{D}$. The orbit contains a sequence of states (or state vectors) that follow from u_0 .

In this article we shall respectively refer (2.1) and (2.2) as discretized elliptic and parabolic PDEs, although they can represent more general parameterized PDEs. In order to use the same framework to study (2.1) and (2.2), we use τ to represent μ in (2.1) and to represent (t, μ) in (2.2). Let \mathcal{T} denote the input space, and $\mathcal{T} = \mathcal{D}$ or $\mathcal{T} = \mathcal{I} \times \mathcal{D}$. Then for both scenarios, $u(\tau)$ and $f(\tau, u)$ could be used to represent the solution snapshot and the vector field corresponding to $\tau \in \mathcal{T}$. It follows that (2.1) and (2.2) become $f(\tau, u) = 0$ and $\dot{u} = f(\tau, u)$ respectively.

An offline-online splitting scheme is used for the model reduction in this article. Let p denote the ensemble size. In the offline stage, $\{\tau_i\}_{i=1}^p$ are sampled in the parameter space, and the corresponding solutions with their derivatives could induce a subspace, where the real solution approximately resides. Induced subspaces in the context of model reduction include the Lagrange, Taylor and Hermite subspaces [?]. In this article, we are focusing on constructing a reduced model in the Lagrange subspace $\mathcal{S}_r = \text{span } \{u_i\}_{i=1}^p \subset \mathbb{R}^n$. The subspace \mathcal{S}_r belongs to the Grassmann manifold $\mathcal{G}_{n,r}$ which is defined as the set of all r -dimensional subspaces of \mathbb{R}^n . The dimension r satisfies $r \leq \min\{n, p\}$. Let $\Phi_r := [\varphi_1, \dots, \varphi_r]$ contains an orthonormal basis $\{\varphi_i\}_{i=1}^r$ of \mathcal{S}_r . Let superscript T denotes matrix transpose, and I_r is the $r \times r$ identity matrix. Then $\Phi_r \in \mathcal{V}_{n,r}$, where $\mathcal{V}_{n,r} = \{A \in \mathbb{R}^{n \times r} | A^T A = I_r\}$ is denoted as the Stiefel manifold of orthonormal r -frames in \mathbb{R}^n . When $r \approx n$, a reduced equation constructed in \mathcal{S}_r could not obtain significant speedups. One often seeks a $k (\ll r)$ -dimensional linear subspace $\mathcal{S}_k \subset \mathcal{S}_r$ where most solution vectors approximately reside. Moreover, there exists an $n \times k$ matrix $\Phi_k = [\phi_1, \dots, \phi_k] \in \mathcal{V}_{n,k}$ whose column space is \mathcal{S}_k . Once the subspace is specified, a reduced model can be constructed by several approaches, such as Galerkin projection [?], Petrov-Galerkin projection [?], and empirical interpolation [?, ?].

3. A General Error Analysis of Reduced Equations. Regardless of the techniques applied for model reduction, a key consideration is how to approximate the original system with high accuracy. In this section, we shall give a general error analysis for the projection-based reduced models.

Using the notations from the previous section, the projection of a state variable $u \in \mathbb{R}^n$ onto \mathcal{S}_r and \mathcal{S}_k can be respectively presented by $\tilde{u}_r := \Phi_r \Phi_r^T u$, and $\tilde{u}_k := \Phi_r \Phi_k^T u$. Let $e_r := u - \tilde{u}_r$ denote the difference between a solution vector u and its projection on \mathcal{S}_r , and $e_k := u - \tilde{u}_k$ denote the difference between u and its projection on \mathcal{S}_k . In addition, we define $e_o := \tilde{u}_r - \tilde{u}_k$ as the difference between these two projections of u .

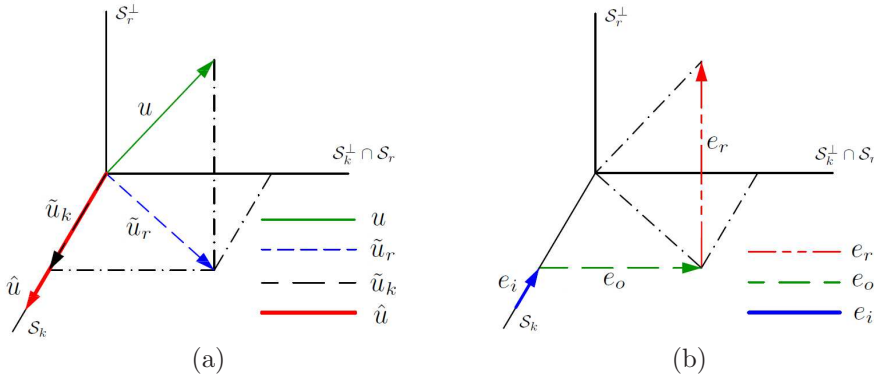


FIGURE 3.1. (Color online.) (a) Illustration of the actual solution u for the original system, the projection \tilde{u}_r of u on \mathcal{S}_r , the projection \tilde{u}_k of u on \mathcal{S}_k and the approximating solution \hat{u} computed by a reduced model. (b) The component of error orthogonal to \mathcal{S}_r is given by $e_r = u - \tilde{u}_r$, the difference of two projections of u is given by $e_o = \tilde{u}_r - \tilde{u}_k$, and the component of error parallel to \mathcal{S}_k is given by $e_i = \tilde{u}_k - \hat{u}$.

Suppose the reduced model has a unique solution, \hat{u} , and $\hat{u} = \hat{u}(\tau) \in \mathcal{S}_k$. Usually, $\tilde{u}_k \neq \hat{u}$, and we use $e_i := \tilde{u}_k - \hat{u}$ to represent their difference. Moreover, numerical simulation inevitably introduces further the numerical error e_t , such as discretization of time integration and the round-off error. This kind of error exists for both high dimensional and low dimensional simulations. However, for simplicity we assume the solution to the reduced model \hat{u} is obtainable by an accurate numerical scheme, and neglect e_t . Using \mathcal{S}_r^\perp and \mathcal{S}_k^\perp to represent the orthogonal complement of subspaces \mathcal{S}_r and \mathcal{S}_k of \mathbb{R}^n , figure 3.1(a) shows u , its projections \tilde{u}_r , \tilde{u}_k , and its approximation from a reduced model \hat{u} . Figure 3.1(b) shows the different components, e_r , e_o , e_i , of error from a reduced model, defined by $e := u - \hat{u}$.

LEMMA 3.1. *The total error e of the approximating solution \hat{u} from a reduced equation, can be decomposed into three components: $e = e_r + e_o + e_i$, and these components are orthogonal to each other.*

Proof. By the definitions of e , e_r , e_o , and e_i , we immediately obtain

$$(3.1) \quad e = u - \hat{u} = (u - \tilde{u}_r) + (\tilde{u}_r - \tilde{u}_k) + (\tilde{u}_k - \hat{u}) = e_r + e_o + e_i.$$

Since $\tilde{u}_r \in \mathcal{S}_r$, $\tilde{u}_k \in \mathcal{S}_k \subset \mathcal{S}_r$, we have $e_o = \tilde{u}_r - \tilde{u}_k \in \mathcal{S}_r$. It follows that there exists a vector $a \in \mathbb{R}^r$ such that $e_o = \Phi_r a$. On the other hand,

$$e_r = u - \tilde{u}_r = (I_r - \Phi_r \Phi_r^T) u.$$

Then the inner product gives

$$(3.2) \quad (e_o, e_r) = a^T \Phi_r^T (I_r - \Phi_r \Phi_r^T) u = a^T (\Phi_r^T - I_r \Phi_r^T) u = 0.$$

Since $\tilde{u}_k, \hat{u} \in \mathcal{S}_k$, one could write $e_i = \tilde{u}_k - \hat{u} = \Phi_k b$ for a vector $b \in \mathbb{R}^k$. Since $\mathcal{S}_k \subset \mathcal{S}_r$, it follows that $(\Phi_r \Phi_r^T) \Phi_k = \Phi_k$. Then the inner product gives

$$(3.3) \quad (e_i, e_r) = b^T \Phi_r^T (I_r - \Phi_r \Phi_r^T) u = b^T (\Phi_r^T - (\Phi_r \Phi_r^T \Phi_k)^T) u = 0.$$

Similarly, by the definition of \tilde{u}_k , we have

$$e_k = u - \tilde{u}_k = (I_k - \Phi_k \Phi_k^T) u.$$

Then the inner product gives

$$(3.4) \quad (e_i, e_k) = a^T \Phi_r^T (I_k - \Phi_k \Phi_k^T) u = a^T (\Phi_k^T - I_k \Phi_k^T) u = 0.$$

On the other hand,

$$(3.5) \quad e_k = u - \tilde{u}_k = u - \tilde{u}_r + \tilde{u}_r - \tilde{u}_k = e_r + e_o.$$

e_o could be considered as the projection of e_k onto the orthogonal complement of \mathcal{S}_k as a subspace of \mathcal{S}_r . Using (3.3), (3.4) and rewriting (3.5) as $e_o = e_k - e_r$, one obtains

$$(3.6) \quad (e_i, e_o) = (e_i, e_k - e_r) = (e_i, e_k) - (e_i, e_r) = 0.$$

A combination of (3.2), (3.3) and (3.6) concludes e_r, e_o, e_i are orthogonal to each other. Moreover, e_k and e_i are orthogonal to each other. \square

Decreasing the magnitude of the projection error $e_k (= e_r + e_o)$ is the key to decrease the total error $e (= e_k + e_i)$. On one hand, e_k provides a lower bound for the reduced model, as $\|e_k\| \leq \|e\|$ is always satisfied. On the other hand, for both elliptic [?] and parabolic PDEs [?], if the Galerkin method is used to produce the reduced equation, there respectively exist a constant C such that $\|e\| \leq C \|e_k\|$. Therefore, a upper error bound of e is also related to e_k . The first component e_r of e_k is directly related to sampling input parameters during the offline stage. One could use uniform sampling process in the parameter space, or use nonuniform sampling process through a greedy algorithm [?, ?]. The second component e_o of e_k comes from the error of dimensionality reduction. If the global POD method is used, then e_o is related to the truncation of the SVD. In this article we are about to discuss an adaptive method to form a reduced subspace \mathcal{S}_k such that $\|e_o\|$ could reach a lower value with fixed k . We will begin with a brief review of POD, which pave a way to introduce the adaptive reduced model.

4. Proper Orthogonal Decomposition (POD). In this section, we give a brief overview of the procedure and properties of POD. In a finite dimensional space, it is essentially the same as the singular value decomposition (SVD). Let $X = [u_1, \dots, u_p]$ be a $n \times p$ snapshot matrix, where each column $u_i = u(\tau_i)$ represents a solution snapshot corresponding to input parameters τ_i . The POD method constructs a basis matrix $\Phi_k \in \mathcal{V}_{n,k}$ that solves the following minimization problem

$$(4.1) \quad \min_{\Phi_k \in \mathcal{V}_{n,k}} \|(I - \Phi_k \Phi_k^T) X\|_F.$$

Thus, the basis matrix Φ_k minimizes the Frobenius norm of the difference between X with its projection $\tilde{X} := \Phi_k \Phi_k^T X$ onto \mathcal{S}_k . Since the dimension of the Lagrange subspace \mathcal{S} is r , it follows that $\text{rank}(X) = r$. Thus, the SVD of X gives

$$(4.2) \quad X = V \Lambda W^T,$$

where $V \in \mathcal{V}_{n,r}$, $W \in \mathcal{V}_{p,r}$, and $\Lambda = \text{diag}(\lambda_1, \dots, \lambda_r) \in \mathbb{R}^{r \times r}$ with $\lambda_1 \geq \lambda_2 \geq \dots \geq \lambda_r > 0$. The λ s are called the singular values of X . In many applications, the truncated SVD is more economical, where only the first k columns V' of V and the first k columns W' of W corresponding to the diagonal matrix Λ' corresponding to the k largest singular values are calculated, and the rest of the matrix is not computed. Then the projection of X is given by

$$(4.3) \quad \tilde{X} = V' \Lambda' W'^T,$$

and the solution of Φ_k in (4.1) is given by $\Phi_k = V'$. Moreover, the projection error of (4.1) in Frobenius norm by the POD method is given by

$$(4.4) \quad E_k = \|(I - \Phi_k \Phi_k^T) X\|_F = \sqrt{\sum_{i=k+1}^r \lambda_i^2}.$$

The key of POD and other projection based reduced models is to find a k -dimensional subspace \mathcal{S}_k on which all the state vectors live. Although the truncated SVD is no longer an exact decomposition of the original matrix X , but it provides the best approximation \tilde{X} to the original data X with least Frobenius norm under the constraint that $\dim(\tilde{X}) = k$. In the rest of this paper, the SVD refers to the truncated SVD unless specified otherwise.

4.1. Galerkin Projection. Let $v_k \in \mathbb{R}^k$ denote the state variable in the subspace coordinate system, and $\hat{u}_k = \Phi_k v_k$ denote the same state in the original coordinate system. Projecting the system (2.1) onto \mathcal{S}_k , one obtains the reduced model of an elliptic PDE,

$$(4.5) \quad \Phi_k^T f(\tau, \Phi_k v_k) = 0,$$

where $\tau = \mu \in \mathcal{D}$ denotes the input parameter. Analogously, a reduced model of a parabolic PDE can be obtained by projecting the system (2.2) on to \mathcal{S}_k ,

$$(4.6) \quad \dot{v}_k = \Phi_k^T f(\tau, \Phi_k v_k),$$

and $\tau = (t, \mu) \in \mathcal{I} \times \mathcal{D}$ is used to identify the solution trajectory corresponding to μ at time t .

Equations (4.5) and (4.6) are reduced equations formed by Galerkin projection. In fact, they can achieve fast computation only when the analytical formula of the reduced vector field $\Phi_k^T f(\tau, \Phi_k v_k)$ can be significantly simplified, especially when it is a linear (or a polynomial) function of v . Otherwise, one need to compute the state variable in the original system $\Phi_k v$, evaluate the nonlinear vector field f at each element, and then, project f onto \mathcal{S}_k . In this case, the reduced models (4.5) and (4.6) are more expensive than the correspondingly full models. To this effect, the discrete empirical interpolation method (DEIM) [?] is proposed to decrease the complexity of computing the nonlinear vector field.

4.2. Discrete Empirical Interpolation Method (DEIM). The original vector field, $f(\tau, u)$ can be split into a linear part and a nonlinear part, i.e.,

$$(4.7) \quad f(\tau, u) = L(\tau)u + N(\tau, u).$$

Using the Galerkin projection, the reduced vector field can be written as

$$(4.8) \quad \Phi_k^T f(\tau, \Phi_k v_k) = \hat{L}v_k + \Phi_k^T N(\tau, \Phi_k v_k),$$

where $\hat{L}(\tau) = \Phi_k^T L \Phi_k$ is a linear operator and $\Phi_k^T N(\tau, \Phi_k v_k)$ denotes the nonlinear term of the vector field. Unless the nonlinear term can be analytically simplified, its computational complexity still depends on n . An effective way to overcome this difficulty is to approximate the nonlinear term by projecting it onto a subspace with much lower dimension. Considering u is a smooth function of τ , we can define a *nonlinear snapshot* $g(\tau) =: N(\tau, u(\tau))$ for $\tau \in \mathcal{T}$. Then the reduced vector field from (4.7) restricted on $\tau \in \mathcal{T}$ and $u = u(\tau)$ can be approximated as

$$(4.9) \quad \Phi_k^T f(\tau, u(\tau)) = \hat{L}v_k + [\Phi_k^T \Psi(P^T \Psi)^{-1}][P^T g(\tau)],$$

where Ψ denotes the collateral POD basis based on a pre-computed nonlinear snapshot ensemble, and P^T is the $n \times d$ index matrix to project a vector of dimension n onto its d elements. For example, if $g = [g_1, \dots, g_4]^T$, and $P^T = [1 \ 0 \ 0 \ 0; \ 0 \ 0 \ 1 \ 0]$, then $P^T g = [g_1, g_3]$. P can be computed by an offline greedy algorithm. We recommend readers to refer [?] for more details. Notice that $\Phi_k^T \Psi(P^T \Psi)^{-1}$ is calculated only once at the outset and $P^T g(\tau)$ is only evaluated on d elements of $g(\tau)$, therefore it is very efficient when $d \ll n$. Using the POD-DEIM approach, we will respectively study nonlinear elliptic and parabolic PDEs in the next two sections.

5. Nonlinear Elliptic PDEs. We are focusing on model reduction for elliptic nonlinear PDEs in this section. The algorithms in this section could be considered as an order-reduced extension for the chord method. We follow the offline-online splitting computational strategy, and use the discrete empirical interpolation method (DEIM) to treat nonlinear terms in the original system.

The general form of elliptic PDEs, after discretization, is given by a nonlinear algebraic equations (2.1). Let p denote the ensemble size. In the offline stage, $\{\mu_i\}_{i=1}^p$ are sampled in the parameter space, and we solve the corresponding solutions $\{u_i\}_{i=1}^p$. If $u_i = u(\mu_i)$ satisfies (2.1), and the Jacobian matrix $J_i := D_u f(\mu_i, u_i)$ is nonsingular, then by the implicit function theorem, there exists neighborhoods $V_i \subset \mathbb{R}^m$ of μ_i , and $U_i \subset \mathbb{R}^n$ of u_i and a smooth map $u : V_i \rightarrow U_i$ such that locally, (2.1) has a unique solution. For a new fixed parameter $\mu_* \in \cap_i V_i$, the following equation has a unique solution,

$$(5.1) \quad F(u) = 0,$$

where $F(u) := f(\mu_*, u)$. Newton iteration and its variations are the most efficient methods known for solving systems of non-linear equations. The most expensive procedures of the standard Newton iteration are to compute the $n \times n$ Jacobian matrix F' for each iteration. Unless an analytical form of F' could be obtained explicitly, evaluation of F' by finite difference method costs n times an evaluation of F because each column in F' requires an evaluation of F .

Motivated by this fact, chord iteration computes $J_0 = F'(u(0))$ at the outset, and use J_0 to approximate the Jacobian for each iteration. Specifically, for iteration j , we

first compute the vector $F(u(j))$. Then, solve

$$(5.2) \quad J_0 \xi(j) = -F(u(j))$$

for $\xi(j)$. After that, update the approximating solution,

$$(5.3) \quad u(j+1) = u(j) + \xi(j).$$

Under certain conditions, the chord iteration could obtain a convergent solution if the initial trial solution is close enough to the actual solution, as given by the following theorems.

THEOREM 5.1. *Suppose (5.1) has a solution u_* , F' is Lipschitz continuous with Lipschitz constant γ , and $F'(u_*)$ is nonsingular. Then there are $\bar{K} > 0$, $\delta > 0$, and δ_1 such that if $u(j) \in \mathcal{B}_{u_*}(\delta)$ and $\|\Delta(u(j))\| < \delta_1$ then*

$$(5.4) \quad u(j+1) = u(j) - (F'(u(j)) + \Delta(u(j)))^{-1}(F(u(j)) + \epsilon(u(j)))$$

is defined and satisfies

$$(5.5) \quad \|e(j+1)\| \leq \bar{K}(\|e(j)\|^2 + \|\Delta(u(j))\| \|e(j)\| + \|\epsilon(u(j))\|),$$

where $e(j) := u_* - u(j)$ denotes the error for iteration j .

For chord iteration, $\epsilon(u(j)) = 0$, $\Delta(u(j)) = F'(u_0) - F'(u(j))$. If $u_0, u(j) \in \mathcal{B}_{u_*}(\delta)$, $\|\Delta(u(j))\| \leq \gamma \|u_0 - u(j)\| \leq \gamma (\|e(0)\| + \|e(j)\|)$. Using theorem 5.1, the following theorem is obtained, where $K_C := \bar{K}(1 + 2\gamma)$.

THEOREM 5.2. *Let the assumptions of theorem 5.1 hold. Then there are $K_C > 0$ and $\delta > 0$ such that if $u_0 \in \mathcal{B}_{u_*}(\delta)$ the chord iteration converges linearly to u_* and*

$$(5.6) \quad \|e(j+1)\| \leq K_C \|e(0)\| \|e(j)\|.$$

We suggest readers to refer to [?] for proofs and more details. For chord method, the complexity of (5.2), (5.3), and direct evaluating $F(u)$ depends on n . If the dimension n in (5.1) is very large, chord iteration could be still prohibitively expensive for real time computation. For this reason, a model reduction approach is applied for decreasing the computational cost based on chord method. A manifold learning procedure is used to extract information from the original data. Usually, this procedure is very intensive in exchange for greatly decreased online cost for each new input-output evaluation. In the online stage, a reduced version of the chord method is used to solve for solution. Since the solution can be solved in a low dimensional subspace, the complexity of online computation can be very low.

5.1. Model Reduction for Chord Iteration. In the offline stage, for each input μ_i , the solution snapshot u_i , the nonlinear snapshot g_i , and the corresponding Jacobian matrix J_i are recorded to form an ensemble $\{\mu_i, u_i, g_i, J_i\}_{i=1}^p$. In the offline stage, we can use POD-Galerkin approach or POD-DEIM to accelerate the computation.

As described in section 4, using the SVD, we can obtain the POD basis matrix Φ_k for the solution snapshots $X = [u_1, \dots, u_p]$ and collateral basis matrix Ψ for the nonlinear snapshots $X' = [g_1, \dots, g_p]$. Let $v(j) \in \mathbb{R}^k$ be the reduced state at iteration j , $J_0 = F'(u_0)$ be the Jacobian at the trial solution, $\hat{J}_0 = \Phi_k^T J_0 \Phi_k \in \mathbb{R}^{k \times k}$ be

the projection of Jacobian J_0 onto \mathcal{S}_k . The Galerkin projection can be used to form reduced equations for (5.2) and (5.3) in chord method,

$$(5.7) \quad \hat{J}_0 \hat{\xi}(j) = -\Phi_k^T F(\Phi_k v(j)),$$

$$(5.8) \quad v(j+1) = v(j) + \hat{\xi}(j).$$

When J_0 is a symmetric positive definite (SPD) matrix, \hat{J}_0 is a nonsingular matrix and (5.7) is well-defined [?]. Moreover, it minimizes the mean square error in the search direction for each iteration. Unfortunately, the Jacobians of a nonlinear problem are not in general SPD matrices and \hat{J}_0 defined above could be singular. One efficient way is to partition the whole parameter domain into some subdomains. For one subdomain, one could pick one parameter, say μ_q , in $\{\mu_i\}_{i=1}^p$ and compute the Jacobian J_q as well as its projection \hat{J}_q onto J_k . If \hat{J}_q is (near) singular, one can choose another parameter in the same subdomain and the reduced Jacobian is nonsingular. Consequently, in the oneline stage, one can directly set \hat{J}_0 from the recorded $\{\hat{J}_q\}$ in the ensemble.

As mentioned in the previous section, POD-Galerkin approach cannot effectively reduce the complexity for high dimensional systems when a general nonlinearity is present, since the cost of computing $\Phi_k^T F(\Phi_k v)$ depends on the dimension of the original system. In order to obtain significant speedups for a general nonlinear system, the DEIM is used to form the reduced version of chord iteration, as shown in algorithm 1. An ensemble $\{\mu_i, u_i, g_i, J_i\}_{i=1}^p$ is pre-computed offline. The POD basis and the collateral POD basis are respectively computed in steps 1 and 2. Some matrices for DEIM is pre-computed in step 3. Step 4 involves parameter domain partition. We use uniform partition in the following simulations. But the algorithm here does not preclude nonuniform partitions. For each subdomain, we choose a reference parameter μ_q and compute and the reduced Jacobian \hat{J}_q and the reduced state v_q .

In the online stage, step 6 requires computing the distance from new input parameter μ_* to each reference parameters in the ensemble. Typically the dimension of parameter space is much lower than the dimension of state variable. In this case, this step is very cheap. Step 7 simply picks up the trial solution and the estimated Jacobian computed in step 5 during the offline stage. Step 6 and 7 are carried out only once. Steps 8-10 in the main loop are carried out in the subspace and their complexity is independent of n . Therefore, the online computation of algorithm 1 is very efficient.

Fixed τ in (4.5), the reduced algebraic equation formed by the Galerkin projection is given by

$$(5.9) \quad \Phi_k^T F(\Phi_k v) = 0.$$

Usually, the reduced chord iteration could not converges to the actual solution, v_* , of (5.9) since DEIM provides an extra error for the approximation for the vector field. However, suppose the DIEM approximation gives a uniform error bound, ϵ_F , for an interested domain of u , an error bound of algorithm 1 could be obtained in terms of ϵ_F . We slightly abuse the notation and use e to dentate the error between v_* and the approximating solution in reduced chord iteration.

THEOREM 5.3. *Suppose (5.9) has a solution v_* , F' is Lipschitz continuous with Lipschitz constant γ , and $F'(\Phi_k v_*)$ is nonsingular. The DIEM approximation gives*

Algorithm 1 Reduced Chord method

Require: Pre-computed ensemble $\{\mu_i, u_i, g_i, J_i\}_{i=1}^p$.

Ensure: Solution u_* that satisfies $F(u) = 0$.

Offline:

1: Use the SVD to compute the global POD basis Φ_k for solution snapshots $\{u_i\}_{i=1}^p$.

2: Use the SVD to compute the globally collateral POD basis Ψ for nonlinear term $\{g_i\}_{i=1}^p$.

3: Use the DEIM to compute $\tilde{L} = \Phi_k^T L \Phi_k$ for linear operator and $\Phi_k^T \Psi (P^T \Psi)^{-1}$ for nonlinear term.

4: Partition the parameter space into p' subdomains.

5: For each subdomain, choose a reference parameter μ_q such that reduced Jacobian $\hat{J}_q = \Phi_k^T J_q \Phi_k$ is nonsingular. Compute solution snapshots in the reduced coordinate system $v_q = \Phi_k^T u_q$.

Online:

6: In the parameter space, compute the distance $d_q = \|\mu_* - \mu_q\|$ from the new parameter μ_* to each reference parameter μ_q .

7: Pick up μ_q with minimal distance, and set v_q as the initially trial solution $v(0)$ in the reduced coordinate system and set \hat{J}_q as the approximation of Jacobian \hat{J}_0 .

for $j = 0, \dots$, (until convergence) **do**

8: Compute $\Phi_k^T \hat{F}(\Phi_k v(j))$, where \hat{F} is an approximation of F by DEIM.

9: Solve $\hat{J}_0 \hat{\xi}(j) = -\Phi_k^T F(\Phi_k v(j))$, as (5.7).

10: Update $v(j+1) = v(j) + \hat{\xi}(j)$, as (5.8).

end for

11: Set $\hat{u}_* = \Phi_k v(j+1)$.

a uniform error bound $\|F(u) - \hat{F}(u)\| < \epsilon_F$ for any $u \in \mathcal{B}_{\Phi_k v_*}$, then there are $\bar{K} > 0$, $K_C > 0$, $\delta > 0$ such that if $u_q \in \mathcal{B}_{\Phi_k v_*}(\delta)$ the reduced chord iteration approach to v_* with the error bound of $\|e(j)\|$ given by $\bar{K} \varepsilon_F / (1 - K_C \delta)$ as $j \rightarrow \infty$ where $e(j) := v_* - v(j)$ denotes the error for iteration j .

Proof. In algorithm 1, a sequence $\{v(j)\}$ is obtained by the following iteration rule,

$$(5.10) \quad v(j+1) = v(j) - \hat{J}_0^{-1}(\Phi_k^T \hat{F}(\Phi_k v(j))),$$

where $\hat{J}_0 = \Phi_k^T J_q \Phi_k$ for $J_q = F'(u_q)$. The above equation could be rewritten in the form similar to (5.4),

$$(5.11) \quad v(j+1) = v(j) - (\Phi_k^T F'(\Phi_k^T v(j)) + \Delta(v(j)))^{-1}(\Phi_k^T F(\Phi_k v(j)) + \epsilon(v(j))),$$

where $\epsilon(v(j)) = \Phi_k^T \hat{F}(\Phi_k v(j)) - \Phi_k^T F(\Phi_k v(j))$, and $\Delta(v(j)) = \hat{J}_0 - \Phi_k^T F'(\Phi_k v(j)) \Phi_k$.

If $u_q, \Phi_k v(j) \in \mathcal{B}_{u_*}(\delta)$, one obtains $\|\epsilon(v(j))\| \leq \|\hat{F}(\Phi_k v(j)) - F(\Phi_k v(j))\| < \epsilon_F$, and $\|\Delta(v(j))\| \leq \|F'(u_q) - F'(\Phi_k v(j))\| \leq \gamma(\|e_q\| + \|e(j)\|)$. Using theorem 5.1, and define $K_C := \bar{K}(1 + 2\gamma)$, one obtains

$$(5.12) \quad \|e(j+1)\| < \bar{K} \|e(j)\| (\gamma \|e_q\| + (1 + \gamma) \|e(j)\|) + \bar{K} \varepsilon_F \leq K_C \delta \|e(j)\| + \bar{K} \varepsilon_F.$$

Let δ small enough such that $K_C \delta < 1$. It follows that $\|e(j)\|$ is bounded by $\bar{K} \varepsilon_F / (1 - K_C \delta)$ as $j \rightarrow \infty$. \square

The reduced chord iteration inherits one advantage of the standard chord iteration, i.e., it does not need compute the Jacobian at each iteration. Therefore, the

per-iteration cost of this method is lower than the cost from a reduced model formed by Newton iteration. On the other hand, an reduced Newton iteration cannot has quadratic convergence rate since the approximation error of the Jacobian matrix or the vector field is inevitable. Therefore, the reduced chord iteration is more efficient for solving the large-scale nonlinear algebraic equation in the context of on line computation.

Notice that if the error bound of DEIM approximation, ε_F in (5.12), approaches zero, the reduced chord iteration converges linearly to v_* . Moreover, ε_F is bounded by a constant times $\|(I - \Psi\Psi^T)F\|$ [?], which indicates an optimal collateral subspace is desired to decrease ε_F . For a fixed dimension k , the following section discuss how to generate optimal subspaces for the solution snapshots and the nonlinear snapshots.

5.2. Adaptive Reduced Model. We consider three SVD-based approaches to construct a subspace \mathcal{S}_k from \mathcal{S}_r . The first approach is the standard POD method, which constructs a *global reduced model* (GRM) from all the solution snapshots in the ensemble. Defining a matrix of p snapshots

$$(5.13) \quad X = [u_1, \dots, u_p],$$

then \mathcal{S}_k is spanned by the columns of the POD basis matrix Φ_k . The projection error of X in Frobenius norm is given by (4.4). This method is straightforward for application, however, if the problem depends on many parameters or if the solution shows a high variability with the parameters, a relatively high dimensional reduced space is needed in order to represent all possible solution variations well. This effect is even considerably increased when treating evolution problems with significant solution variations in time. Another aspect is the fact that projection based model reduction techniques, such as POD, usually generate small but full matrices while common discretization techniques (such as finite difference) could lead to large but sparse matrices. Unless the reduced model has significantly lower dimension, it is even possible that the reduced model is more time consuming than the original model.

The second approach is the *local reduced model* (LRM), which partitions the interested parameter domain into some disjoint subregions and forms a local snapshot matrix for each subregion. Suppose μ_* resides on a subregion that contains l input parameters $\{\mu_i | i \in \mathcal{D}^L\}$ in the ensemble, where $\mathcal{D}^L = \{k_1, k_2, \dots, k_l\} \subset \{1, 2, \dots, p\}$, then the local snapshot matrix can be set as

$$(5.14) \quad X^L = [u_{k_1}, \dots, u_{k_l}].$$

The supper script L denotes the LRM. Since X^L contains less snapshots than X , it is expected that the LRM needs lower dimension to approximate the original system. Equivalently, if the LRM has the same dimension as the GRM, it has less truncation error during the SVD process. On the other hand, since the LRM does not use solution snapshots in some other partitioned subregions, it may not be able to obtain an approximating solution with high-order accuracy.

We extend the idea of the LRM and propose the third approach for model reduction, the *adaptive reduced model* (ARM), to compute the adaptive reduced bases for parameter variation. Similar to LRM, we first partition the interested parameter domain into some subregions, and determine one subregion that μ_* resides. The reference solution snapshot u_q for this subregion could be approximated by a linear combination $u_q \approx \sum_{i=1}^p a_i(\mu_q)u_i$ of all the solution snapshots in the ensemble, where the interpolation coefficient $a_i(\mu_q)$ is a function on the parameter space,

and satisfies $0 \leq a_i \leq 1$. For example, it could be set as a Gaussian function $a_i(\mu_q) = C_0 \exp(-\|\mu_i - \mu_q\|^2/2\sigma^2)$, with the normalized coefficients C_0 and the kernel length σ . σ should be larger than the maximal radius of all the subregions.

If μ_q is a close enough to μ_* , we can estimate an approximation of $u(\mu_*)$, or its projection \tilde{u}_r , through a variation of μ_q

$$(5.15) \quad \tilde{u}_r^A = \sum_{i=1}^p (1 + \eta_i) a_i u_i,$$

where $[\eta_1, \dots, \eta_p]^T \in \mathcal{B}_0(\epsilon_\eta)$, and $\eta_i = 0$ for all i if $a_i = 0$. Let $\mathcal{S}_r^A = \text{span}\{a_i u_i\}_{i=1}^p$ denote a new Lagrange subspace in \mathcal{S}_r . Using superscript A to denote the proposed ARM, a weighted snapshot matrix for the subregion that μ_* resides can be defined as

$$(5.16) \quad X^A = [a_1 u_1, a_2 u_2, \dots, a_p u_p].$$

Let $r^A = \det(X^A)$, obviously we have $r^A \leq r$. When $r^A > k$, the SVD can be used to extract the first k dominant modes from X^A , and obtain a subspace \mathcal{S}_k^A in \mathcal{S}_r^A . Let column vectors of $\Phi_k^A \in \mathcal{V}_{n \times k}$ span \mathcal{S}_k^A . As an analogy of E_k in (4.4), the projection error of X^A onto \mathcal{S}_k^A in Frobenius norm is given by

$$(5.17) \quad E_k^A = \left\| (I_k - \Phi_k^A (\Phi_k^A)^T) Y \right\|_F = \sqrt{\sum_{i=k+1}^r (\lambda_i^A)^2},$$

where λ_i^A is the i th singular value of X^A . When $r^A \leq k$, the SVD or the Gram-Schmidt process could be used to obtain r^A orthonormal bases that span \mathcal{S}_r^A . Choose any additional $k - r^A$ vectors to form an $n \times k$ matrix $\Phi_k^A \in \mathcal{V}_{n \times k}$, (5.17) becomes $E_k^A = 0$. Comparing E_k with E_k^A , we have the following lemma.

LEMMA 5.4. *Let X and X^A be the matrices for solution snapshots and weighted solution snapshots. E_k and E_k^A are projection errors respectively given by (4.4) (5.17). Then, $E_k \geq E_k^A$.*

Proof. When $r^A \leq k$, the conclusion holds trivially. We consider the case for $r^A > k$. For each weighing coefficient a_i in X^A , we have $0 \leq a_i \leq 1$. It follows that

$$(5.18) \quad \begin{aligned} \left\| (I_k - \Phi_k \Phi_k^T) X \right\|_F &= \left\| (I_k - \Phi_k \Phi_k^T) u_1, \dots, (I_k - \Phi_k \Phi_k^T) u_p \right\|_F \\ &\geq \left\| (I_k - \Phi_k \Phi_k^T) a_1 u_1, \dots, (I_k - \Phi_k \Phi_k^T) a_p u_p \right\|_F \\ &= \left\| (I_k - \Phi_k \Phi_k^T) X^A \right\|_F \\ &\geq \left\| (I_k - \Phi_k^A (\Phi_k^A)^T) X^A \right\|_F. \end{aligned}$$

The last inequity holds because Φ_k^A provides a least Frobenius norm for the difference of matrix X^A and its projection onto a k -dimensional subspace. Using the definition of E_k and E_k^A , one obtains $E_k \geq E_k^A$. Especially, $E_k = E_k^A$ holds if and only if for any i , $a_i = 1$. In this case, the ARM degenerates to the GRM. \square

COROLLARY 5.5. *Let X and X^L be the matrices for solution snapshots and local solution snapshots. E_k and E_k^L are projection errors. Then, $E_k > E_k^L$.*

Proof. We construct a $n \times p$ matrix $X' = [b_1 u_1, \dots, b_p u_p]$. Let $b_i = 1$ when $i \in \mathcal{D}^L$ and $b_i = 0$ otherwise. Essentially, X' is an extension of X^L with some 0 column vectors. The SVD of X' and X^L gives the same POD basis matrix Φ_k^L and

singular values λ_i^L . Therefore, the projection error in Frobenius norm, E_k^L , is given by $\|(I_k - \Phi_k^L(\Phi_k^L)^T)X'\|_F$. Since $b_i = 0$ for some i , by lemma 5.4, it follows that

$$(5.19) \quad \|(I_k - \Phi_k \Phi_k^T)X\|_F > \|(I_k - \Phi_k^L(\Phi_k^L)^T)X'\|_F.$$

The above equation means $E_k > E_k^L$, i.e., the projection error of the LRM is smaller than the error from the GRM. \square

Lemma 5.4 and corollary 5.5 compare projection error of the same data ensemble $\{u_i\}_{i=1}^p$, and suggests that E_k^A and E_k^L is usually smaller than E_k . Furthermore, for a specified parameter μ_* , if the projection \tilde{u}_r of u_* has a form of (5.15), the SVD truncation error e_o^A of the ARM is bounded by a constant times E_k^A ,

$$(5.20) \quad \begin{aligned} \|e_o^A\| &= \|\tilde{u}_r^A - \tilde{u}_k^A\| = \left\| \sum_{i=1}^p (1 + \eta_i) a_i u_i - (1 + \eta_i) a_i (\Phi_k^A(\Phi_k^A)^T) u_i \right\| \\ &\leq \sum_{i=1}^p \left\| (I - \Phi_k^A(\Phi_k^A)^T) (1 + \eta_i) a_i u_i \right\| \leq \max_i (1 + \eta_i) \sum_{i=1}^p \left\| (I - \Phi_k^A(\Phi_k^A)^T) a_i u_i \right\| \\ &\leq (1 + \epsilon_\eta) E_k^A. \end{aligned}$$

The error bound of e_o of the GRM has the similar property

$$(5.21) \quad \begin{aligned} \|e_o\| &= \|\tilde{u}_r - \tilde{u}_k\| = \left\| \sum_{i=1}^p (1 + \eta_i) a_i u_i - (1 + \eta_i) \eta_i a_i (\Phi_k \Phi_k^T) u_i \right\| \\ &\leq \sum_{i=1}^p \left\| (I - \Phi_k \Phi_k^T) (1 + \eta_i) a_i u_i \right\| \leq \max_i (1 + \eta_i) \|a_i\| \sum_{i=1}^p \left\| (I - \Phi_k \Phi_k^T) u_i \right\| \\ &\leq (1 + \epsilon_\eta) E_k \end{aligned}$$

Combined (5.20) with (5.21), and using lemma (5.4), we conclude that the upper error bound of e_o^A is smaller than e_o , provided that $\tilde{u}_r^A = \Phi_r \Phi_r^T u_*$.

We next consider the projection error e_r of u_* . Since the GRM uses all the solution snapshots to form a snapshot matrix, it immediately follows that $\|e_r\| \leq \|e_r^A\|$, and $\|e_r\| < \|e_r^L\|$. More specifically, suppose the solution u is a smooth function of μ , the Taylor expansion of u at μ_* could be approximated by a linear combination of $\{u_i\}_{i=1}^p$. The first few order terms of the Taylor polynomial could be matched, and the remainders can be expressed by a higher order term. Let m be the dimension of μ , s be the highest order that could be matched, and $\binom{m+s}{s} \leq p$. Since e_r is bounded by all the remainders whose order is no larger than $s+1$, then $\|e_r\| < \min_{i=1}^{s+1} \{c_i(\mu_*) \delta(\mu_*, i)^i\}$, where $c_i(\mu_*)$ denotes the maximal norm of the i th order derivative of u at μ_* , $\delta(\mu_*, i)$ denotes the norm distance from μ_* to its nearest $\binom{m+i}{i}$ neighbors. As more snapshots are counted to form the snapshot matrix, s and $\delta(\mu_*, s)$ increase simultaneously. To this effect, only local snapshots contribute significantly to reduce e_r . The above analysis also applies for the APM and LRM. Therefore, if a noncompact scheme is used for the ARM, $\|e_r^A\|$ could be very close to $\|e_r\|$.

Replacing u_i by g_i , we can use the same procedure to compute the collateral reduced basis for nonlinear snapshots by the SVD from

$$(5.22) \quad Y = [a_1 g_1, \dots, a_p g_p],$$

and then use the reduced chord iteration to find an approximating solution.

5.3. Numerical Example. In this subsection, the adaptive reduced model is applied to an elliptic PDE (from [?] and [?]),

$$(5.23) \quad -\nabla^2 u(x, y) + \frac{\mu_1}{\mu_2}(\mathrm{e}^{\mu_2 u} - 1) = 100 \cos(2\pi x) \cos(2\pi y),$$

with homogeneous Dirichlet boundary conditions, $u(0, y) = u(1, y) = u(x, 0) = u(x, 1) = 0$. The spatial variables $(x, y) \in \Omega = [0, 1]^2$ and the parameters satisfy $\mu = (\mu_1, \mu_2) \in \mathcal{D} = [0.01, 10]^2 \subset \mathbb{R}^2$. The “real” solution is solved by Newton iteration resulting from a finite difference discretization. The spatial grid points (x_i, y_j) are equally spaced in Ω for $i, j = 1, \dots, 50$. The full dimension for the state variable u is then $n = 2500$.

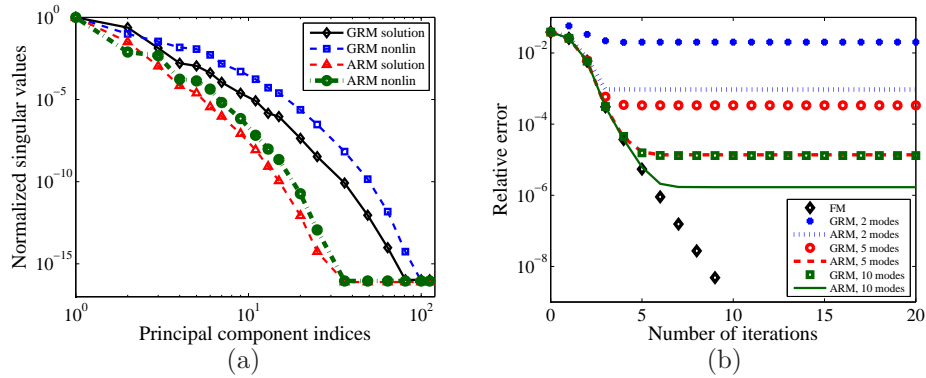


FIGURE 5.1. (Color online.) Simulation results for equation (5.23). (a) Normalized singular values of the matrices of solution snapshots and nonlinear snapshots. The singular values of in the adaptive reduced model (ARM) decrease faster than the corresponding values in the global reduced model (GRM). Singular values of solution matrices decrease faster than the singular values of nonlinear matrices. (b) The relative error for the chord iteration and its reduced model. The full model (FM) is computed by 50×50 grid points. For the reduced model, the POD-DEIM approach is used. We set the subspace dimension for the nonlinear term $s(u, \mu)$ twice as the subspace dimension for the solution u to balance the POD error and the error from DEIM approximation. For both GRM and ARM, solution subspaces are spanned by 2, 5, and 10 modes respectively, and the subspaces for nonlinear term are spanned by 4, 10, 20 accordingly. The relative error is defined as $\|u(\mu) - \hat{u}(\mu)\| / \|u(\mu)\|$

Figures 5.1(a) shows the normalized singular values for the solution snapshots of (5.23) and nonlinear snapshots $s(u, \mu) = \mu_1/\mu_2(\mathrm{e}^{\mu_2 u} - 1)$ of the uniformly selected 121 input parameters, for the GRM and the ARM discussed in section 5.2. The parameter domain \mathcal{D} is uniformly partitioned into 25 subregions. All the singular values are normalized by the largest one. Compared with GRM, the singular values in ARM has faster decreasing rate, which means in order to obtain the same level of accuracy, ARM needs fewer modes to represent the original system. Figure 5.1(b) shows that the ARM formed by POD-DEIM reduced system can accurately reproduce the solution of the full-order system of dimension 2500 with relative error $\mathcal{O}(10^{-3})$ by 2 modes to approximate solution snapshots, with relative error $\mathcal{O}(10^{-5})$ by 5 modes and with relative error $\mathcal{O}(10^{-6})$ by 10 modes. Since the normalized singular values of the nonlinear snapshots decrease slower than the values of solution snapshots, we set the dimension of collateral subspace twice as the dimension of the solution subspace. As expected, APM has much higher accuracy than GRM for the same dimension. These errors are averaged over a set of 100 parameters μ that were not used to obtain the sample snapshots. This suggests that the POD-DEIM reduced system can give

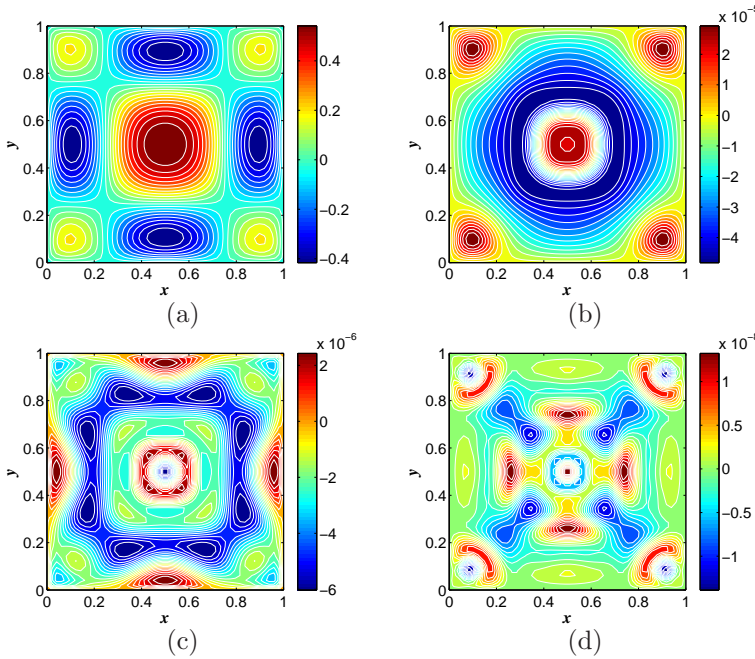


FIGURE 5.2. (Color online.) Simulation results for the elliptic equation (5.23) with $\mu = (\mu_1, \mu_2) = (4.5, 8.5)$. (a) The solution snapshot computed by the full model with $\text{dim} = 2500$. (b) Error $e = u - \hat{u}$ at the grid points with the solution from the POD-DEIM reduced system for solution $\text{dim} = 2$ with nonlinear term $\text{dim} = 4$. (c) Error e for solution $\text{dim} = 5$ with nonlinear term $\text{dim} = 10$. (d) Error e for solution $\text{dim} = 10$ with nonlinear term $\text{dim} = 20$. The reduced model formed by ARM could obtain the same accuracy level in a lower dimensional subspace.

a good approximation to the original system with any value of parameter $\mu \in \mathcal{D}$. Figure 5.2 (a) shows the snapshot corresponding to the input parameters $\mu_1 = 4.5$, and $\mu_2 = 8.5$. Figures 5.2(b)-5.2(d) respectively show the errors at the grid points from the solution of the POD-DEIM reduced system with solution dimension as 2, 5, and 10, respectively.

6. Nonlinear Parabolic PDEs. In this section, we extend our adaptive model reduction approach to treat nonlinear parabolic PDEs. We first introduce the methodology and then illustrate that the proposed method has a high accuracy for the nonlinear Burgers equation.

6.1. Methodology. The general form of parabolic PDEs, after discretization, is given by an ODE (2.2). We still follow the offline-online splitting computational strategy, and use the discrete empirical interpolation method (DEIM) to treat nonlinear terms in the original system.

In the offline computation, for each input parameter μ_i the solution trajectory gives a snapshot matrix $X_i = [u(t_1, \mu_i), \dots, u(t_T, \mu_i)]$. Using the standard SVD, we have $X_i = V_i \Lambda_i W_i^T$, where $V_i = [v_1(\mu_i), \dots, v_{r_i}(\mu_i)]$ is a set of orthonormal bases, $\Lambda_i = \text{diag}\{\lambda_1(\mu_i), \dots, \lambda_{r_i}(\mu_i)\}$ contains the corresponding eigenvalues. The POD bases Φ_i is given by the first k_i columns of V_i . Correspondingly Λ'_i is defined as the first $k_i \times k_i$ block of Λ_i . Then Φ_i minimizes the truncation error of X_i and its projection onto the column space of Φ_i , which is given by $E_i = \|(I - \Phi_i \Phi_i^T) X_i\|_F$.

We shall use adaptive reduced bases to form a reduced model. As an analogy of

(5.16), the weighted snapshot matrix for the ODE, can be defined by

$$(6.1) \quad X^A = [a_1 X_1, \dots, a_p X_p],$$

where $\{a_i\}_{i=1}^p$ are the weighting coefficients for the new parameter μ_* . This is slight different than the weighted snapshot matrix for the elliptic PDEs, where a_i is computed based on a reference point μ_q for a subregion. Usually, time integration for a parabolic equation is much more expensive than a few iterations based on the reduced chord method. On the other hand, the norm error grows exponentially for a parabolic equation, and decreasing the projection error is crucial to limit the total error. Therefore, for parabolic PDEs we can compute the adaptive bases corresponding to μ_* in the online stage; but for elliptic PDEs, we partition the interested parameter region into some subregions and pre-compute the adaptive bases for each subregion in the offline stage. If all a_i s equal 1, the ARM degenerates to the GRM and if a_i is formed by a compact scheme, such as a Gaussian function, it leads to less truncation error during the SVD process. Since this section only discusses the ARM for the parabolic PDEs, we shall remove the superscript A for convenient, and denote X for X^A .

The direct SVD of X could obtain reduced bases, but it is not the most efficient approach. When the trajectories show fast variation over a long time domain, it requires allocating large memory to record X . Suppose we pick T snapshots from each trajectory, then the total size of X is $n \times pT$. If pT is very large, the SVD of X could be expensive. In order to save more memory and improve the efficiency, we define an *information matrix*,

$$(6.2) \quad X' := [a_1 \Phi_1 \Lambda'_1, \dots, a_p \Phi_p \Lambda'_p].$$

If each Φ_k is a $n \times k$ matrix, then the size of \tilde{X} is $n \times pk$. Notice that $k \ll T$ for parabolic PDEs with large time domain. We claim the adaptive reduced bases can be computed by the SVD of \tilde{X} .

THEOREM 6.1. *Let $\Phi \in \mathcal{V}_{n,k'}$ minimize the truncation error of X' and its projection onto a k' -dimensional subspace of \mathbb{R}^n . The error is given by $E_0 = \|(I - \Phi \Phi^T) X'\|_F$ in Frobenius norm. Then the projection error for the original weighted snapshot matrix X in (6.1) is bounded by*

$$(6.3) \quad \|(I - \Phi \Phi^T) X\|_F \leq E_0 + \sqrt{\sum_{i=1}^p a_i^2 E_i^2}.$$

Proof. Since the non-truncated SVD gives $X_i = V_i \Lambda_i W_i^T$, by the definition of X , we have $X = [a_1 V_1 \Lambda_1 W_1^T, \dots, a_p V_p \Lambda_p W_p^T]$. We construct a new matrix

$$\tilde{X} := [a_1 V_1 \tilde{\Lambda}_1 W_1, \dots, a_p V_p \tilde{\Lambda}_p W_p^T],$$

where $\tilde{\Lambda}_i$ is has the same size as Λ_i , but only contains the first k_i nonzero singular values of Λ_i , i.e., $\tilde{\Lambda}_i = \text{diag}\{\lambda_1(\mu_i), \dots, \lambda_{k_i}(\mu_i), 0, \dots, 0\}$. Since W_i are orthonormal,

$$(6.4) \quad (X - \tilde{X})(X - \tilde{X})^T = \sum_{i=1}^p a_i^2 V_i (\Lambda_i - \tilde{\Lambda}_i)^2 V_i^T.$$

It follows that

$$(6.5) \quad \begin{aligned} \|X - \tilde{X}\|_F^2 &= \text{tr} \left((X - \tilde{X})(X - \tilde{X})^T \right) = \sum_{i=1}^p \text{tr} (a_i^2 V_i (\Lambda_i - \tilde{\Lambda}_i)^2 V_i^T) \\ &= \sum_{i=1}^p a_i^2 \text{tr} ((\Lambda_i - \tilde{\Lambda}_i)^2) = \sum_{i=1}^p a_i^2 E_i^2 \end{aligned}$$

The last equity holds because $E_i = \|(I - \Phi_i \Phi_i^T) X_i\|_F = \sqrt{\sum_{j=k_i+1}^{r_i} \lambda_j^2}$. On the other hand,

$$(6.6) \quad \begin{aligned} \|(I - \Phi \Phi^T) \tilde{X}\|_F &= \left\| (I - \Phi \Phi^T) [a_1 V_1 \tilde{\Lambda}_1, \dots, a_p V_p \tilde{\Lambda}_p] \text{diag}\{W_1^T, \dots, W_p^T\} \right\|_F \\ &= \left\| (I - \Phi \Phi^T) [a_1 V_1 \tilde{\Lambda}_1, \dots, a_p V_p \tilde{\Lambda}_p] \right\|_F = \left\| (I - \Phi \Phi^T) [a_1 \Phi_1 \Lambda'_1, \dots, a_p \Phi_p \Lambda'_p] \right\|_F \\ &= \|(I - \Phi \Phi^T) X'\|_F = E_0 \end{aligned}$$

Using (6.5) and (6.6), and combining the following inequity,

$$(6.7) \quad \begin{aligned} \|(I - \Phi \Phi^T) X\|_F &\leq \|(I - \Phi \Phi^T) \tilde{X}\|_F + \|(I - \Phi \Phi^T)(X - \tilde{X})\|_F \\ &\leq \|(I - \Phi \Phi^T) \tilde{X}\|_F + \|X - \tilde{X}\|_F \end{aligned}$$

(6.3) is obtained. \square

We notice that each Φ_i in (6.2) does not necessary to have the same size. Based on the singular values in Λ_i , we can adaptively set k_i such that each E_i is smaller than a constat number, say ϵ_0 , during the offline stage. Moreover, the dimension k' of Φ could also be adaptively chosen such that the total projection error bound, given by the RHS of (6.3), is smaller than another given number.

Similarly the collateral information matrix for the nonlinear snapshots shares the similar expression, i.e.,

$$(6.8) \quad Y' = [a_1 \Psi_1 \Sigma_1, \dots, a_p \Psi_p \Sigma_p],$$

where Ψ_i and Σ_i are computed by the truncated SVD for the nonlinear snapshots on the trajectory $u(\mu_i)$. Having two sets of basis vectors, a reduced equation, formed by POD-Galerkin approach (4.6) or POD-DEIM approximation (4.9), could be used to solve an approximating solution $\hat{u}(t, \mu)$.

Suppose the weighting interpolation coefficients $\{a_i\}_{i=1}^p$ are continuous functions of μ . Then X' in (6.2) could be considered as a continuous matrix-valued function of parameter μ . The truncated SVD is a continuous map from X' to Φ . It follows that the mapping $\mathcal{S} : \mu \mapsto \mathcal{S}(\mu)$ is a continuous function from parameter space to Grassmann manifold. Finally, the solution of a reduced equation $\hat{u}(t, \mu)$ is a smooth function of μ .

6.2. Numerical Example. The proposed algorithm is illustrated in this subsection by testing it to solve the one dimensional Burgers equation, which focuses on demonstrating the capability of adaptive reduced model to deliver accurate results.

Let $u = u(t, x)$. Consider the one-dimensional Burgers equation with constant diffusion coefficient ν ,

$$(6.9) \quad \frac{\partial u}{\partial t} = -u \frac{\partial u}{\partial x} + \nu \frac{\partial^2 u}{\partial x^2},$$

on space $x \in [0, 1]$. Without loss of generality, periodic boundary conditions are applied, with $u(t, 0) = u(t, 1)$, and $u_x(t, 0) = u_x(t, 1)$. The initial condition is provided by a Gaussian function $u(0, x) = \exp(-12.5(x - 1/3)^2)$.

The fully resolved model is obtained through a high resolution finite difference simulation with spatial discretization by $n = 1000$ equally spaced grid points. The time domain for the simulation is set as $[0, 1]$, and the unit time step is 2×10^{-4} . The advection term is discretized by the first-order upwind difference scheme with the forward Euler method for time integration while the diffusion term is discretized by the second-order central difference scheme with the Crank-Nicolson method for time integration.

In the simulation we set the diffusion coefficients ν from 0.001 to 0.01 with equally spaced intervals 0.001. Since states of Burgers equation show a high variability with time evolution, compared with an elliptic equation more modes are needed in order to present the whole solution trajectory with high accuracy. For each trajectory, the first 100 modes with singular values of solution snapshots and the first 150 modes with singular values of nonlinear snapshots are restored. Figures 6.1(a) shows the normalized singular values of the information matrices X' and Y' . All the singular values are normalized by the largest one. The singular values in ARM have faster decreasing rate, which means in order to obtain the same level of accuracy, ARM needs less modes represent the original system. There is a link when the principle component indices are greater than 100 for X' or 150 for Y' , which is due to the truncation from the SVD of the original trajectory in the ensemble. Figure 6.1(b) shows the average norm error for 10 new parameters where the reduced models are formed by the standard Galerkin projection and the DEIM. For the DEIM case, the dimension for nonlinear term subspace is 1.5 times of dimension of the solution subspace. It is noticed that the GRM always has higher truncation error than the ARM for a fixed dimension.

Since the one-dimensional Burgers equation has a positive velocity, a wave will propagate to the right with the higher velocities overcoming the lower velocities and creating steep gradients. This steepening continues until a balance with the dissipation is reached, as shown by the velocity profile at $t = 1$ in Figure 6.2.

7. Conclusion. In this paper, we propose a new method to form adaptive reduced bases for model reduction of large-scale parameterized PDEs. The method could be applied to both elliptic and parabolic PDEs based on the proper orthogonal decomposition (POD) and the discrete empirical interpolation method (DEIM). For elliptic PDEs, the basis vectors of solution subspace and nonlinear term subspace are respectively computed by the singular value decomposition (SVD) of the information matrices, whose columns are defined as the weighted solution snapshots and nonlinear snapshots. The reduced chord iteration is formulated using the adaptive reduced bases. For parabolic PDEs, the information matrices for solution subspace and nonlinear term subspace are respectively computed from a set of empirical eigenfunctions times the corresponding empirical eigenvalues from the pre-computed trajectories. Both Analytical results and numerical simulations demonstrate that the reduced equation corresponding to the adaptive bases can yield much higher accuracy than the classical POD method for the same dimension.

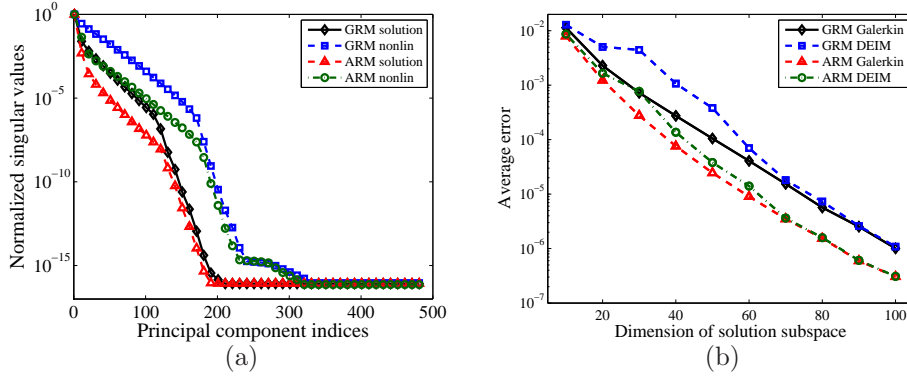


FIGURE 6.1. (Color online.) Simulation results for one-dimensional Burgers equation (6.9). (a) Normalized singular values of the information matrices of solution snapshots and nonlinear snapshots. The singular values of adaptive reduced basis have faster decreasing rate compared with global reduced basis. Meanwhile, the singular values of solution matrices decrease faster than the singular values of nonlinear matrices. (b) The error for the ARM and the GRM obtained by the Galerkin projection and the DEIM. Plot of the maximal difference between the benchmark solution $u(t)$ and the approximating solution $\hat{u}(t)$, $\|e\|_\infty = \sup\{\|u_*(t) - \hat{u}(t)\|_\infty : t \in [0, 0.1]\}$. One on hand, reduced model formed by the DEIM could be a good approximation for the Galerkin projection, especially when the dimension increases. One the other hand, for the same dimension, the ARM could always obtain higher accuracy compared with the GRM.

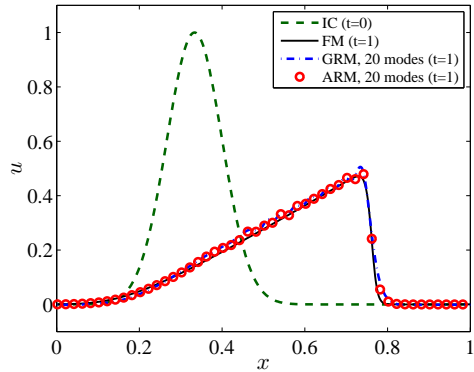


FIGURE 6.2. (Color online.) Simulation results for one-dimensional Burgers equation (6.9) with fixed space domain $[0, 1]$. The velocity profiles at $t = 0$ and $t = 1$ with constant diffusion coefficient $\nu = 1.5 \times 10^{-3}$. 1000 grid points are used to obtain the full model (FM). For the GRM and the ARM, the solution is obtained from the POD-DEIM reduced system for solution dim = 20 with nonlinear term dim = 40.